الجمهورية الجزائرية الديمقراطية الشعبية
THE PEOPLE'S DEMOCRATIC REPUBLIC OF ALGERIA
وزارة التعليم العالي والبحث العلمي
THE MINISTRY OF HIGHER EDUCATION AND SCIENTIFIC RESEARCH
جامعة عمّار ثليجي بالأغواط
AMAR TELIDJI UNIVERSITY OF LAGHOUAT
كلية التكنولوجيا
FACULTY OF TECHNOLOGY
قسم الالكتروتقني
DEPARTMENT OF ELECTROTECHNIC

Master's dissertation

Domain: Science and Technology
Field: Electrical Engineering
Option: Renewable Energy

By:

LAGGOUN ABDERRAHMANE

THEME

Fault detection based on power losses analysis for enhanced efficiency in sustainable photovoltaic systems

Mr. BESSEDIK Sid Ahmed	*Pr. (President)*
M. BOUCHIBA Oumelkhier	*MCA. (Examiner)*
Mr. BIRANE Mouhoub	*Pr. (Supervisor)*
M.r BENMOUIZA Khalil	*Pr.(co-supervisor)*

Academic year 2024/2025

Abstract:

This dissertation presents a methodology for fault detection in grid-connected photovoltaic (PV) systems based on power loss analysis. A 100 kW PV array was modelled using MATLAB/Simulink to simulate various fault scenarios at the PV array, DC-DC converter, and grid interface levels. By comparing the system's voltage, current, and power outputs under normal and faulty conditions, characteristic fault signatures were identified, enabling accurate and timely diagnosis. The results aim to enhance the reliability and efficiency of large-scale PV installations, reduce unplanned outages, and support the development of resilient renewable energy infrastructures.

Keywords: fault detection, photovoltaic systems, power loss analysis, MATLAB/Simulink schema de blocs, renewable energy

ملخص:

تقدم هذه الأطروحة منهجية للكشف عن الأعطال في أنظمة الطاقة الشمسية المتصلة بالشبكة الكهربائية استنادًا إلى تحليل فقدان الطاقة. تم تصميم مصفوفة شمسية بقدرة 100 كيلوواط باستخدام برنامج MATLAB/Simulinkلمحاكاة سيناريوهات الأعطال المختلفة على مستوى المصفوفة الشمسية، ومحول التيار المستمر(DC-DC) ، وواجهة الشبكة. من خلال مقارنة جهد النظام والتيار ومخرجات الطاقة في الظروف العادية والمعطلة، تم تحديد علامات الأعطال المميزة، مما يتيح التشخيص الدقيق والسريع. تهدف النتائج إلى تعزيز موثوقية وكفاءة المنشآت الشمسية الكبيرة، وتقليل الانقطاعات غير المخطط لها، ودعم تطوير بنى تحتية للطاقة المتجددة أكثر مرونة .

الكلمات المفتاحية: كشف الأعطال، أنظمة الطاقة الشمسية، تحليل فقدان الطاقة، MATLAB/Simulink، الطاقة المتجددة

Résumé :

Cette dissertation présente une méthodologie de détection des défauts dans les systèmes photovoltaïques (PV) connectés au réseau, basée sur l'analyse des pertes de puissance. Un réseau PV de 100 kW a été modélisé à l'aide de MATLAB/Simulink pour simuler divers scénarios de défauts au niveau du réseau PV, du convertisseur DC-DC et de l'interface réseau. En comparant les sorties de tension, de courant et de puissance du système dans des conditions normales et défectueuses, des signatures caractéristiques des défauts ont été identifiées, permettant un diagnostic précis et rapide. Les résultats visent à améliorer la fiabilité et l'efficacité des installations PV à grande échelle, à réduire les pannes imprévues et à soutenir le développement d'infrastructures d'énergie renouvelable plus résilientes.

Mots clés : détection de défauts, systèmes photovoltaïques, analyse des pertes de puissance, MATLAB/Simulink, énergie renouvelable

Acknowledgements

First and foremost, we are very grateful to **ALLAH S.W.T** for giving us the key and opportunity to accomplish our master dissertation.

We would like to express our sincere gratitude to our supervisor, **Pr. Mouhoub Birane**, for his invaluable guidance and support, and for providing helpful feedback and suggestions throughout our master's program. His expertise and encouragement helped us to complete this research and write this dissertation.

We want to thank our co-supervisor, **Pr. BENMOUIZA Khalil**, for his constant support, availability, and valuable advice during the realization of this work.

We are also grateful to the members of the jury for evaluating our work and for their valuable suggestions, which will undoubtedly enrich our academic experience.

Lastly, we would like to express our appreciation to all the professors, administrative staff, and technicians of the Department of Electrical Engineering at **Amar Telidji University of Laghouat** for their support throughout our studies.

Dedication

To my beloved parents,

whose unconditional love, prayers, and sacrifices
have been the foundation of my achievements.

To my teachers, mentors, and friends,

for their guidance, encouragement, and companionship
along the way.

This dissertation is dedicated with deep gratitude and
respect.

Abderrahmane Laggoun

Contents

List of Figures

List of Tables

Nomenclature

α	Duty cycle (alternative notation for D)
$\frac{dP}{dV}$	Power-voltage derivative for MPPT (W/V)
G	Solar irradiance (alternative notation for I_r, W/m^2)
I_L	Light-generated current (equivalent to I_{Ph})
I_{AC}	AC output current (A)
k	Boltzmann's constant (1.381×10^{-23} J/K)
K_i	Integral gain for MPPT controller
n	Diode ideality factor (dimensionless)
q	Elementary charge (1.602×10^{-19} C)
R_{sh}	Shunt resistance (equivalent to R_p)
T	Cell temperature (K)
T_s	Switching period (s)
T_{off}	Switch off-time (s)
T_{on}	Switch on-time (s)
U_{ref}	Reference voltage for VSC control (V)
V_{AC}	AC output voltage (V)
V_{in}	Input voltage to converter (V)
V_{out}	Output voltage from converter (V)

General Introduction

As global energy demand continues to rise amid increasing environmental concerns over the use of fossil fuels, photovoltaic (PV) systems have emerged as a cornerstone of renewable energy production. Their scalability, declining costs, and minimal carbon footprint make them a promising solution for sustainable power generation (1).

However, despite their advantages, PV installations are prone to various types of faults, including cell microcracks, bypass diode failures, and grid-connection issues. These faults can significantly impact system performance, leading to energy losses, decreased operational efficiency, and a reduced system lifespan (2).

This thesis proposes a methodology for detecting faults in grid-connected PV systems by analyzing power losses. A 100 kW PV array is modeled using MATLAB/Simulink to simulate fault scenarios at three critical levels: the PV array, the DC–DC (boost) converter, and the grid interface. Each faulty case is compared against an ideal baseline scenario to identify characteristic signatures in voltage, current, and power outputs, facilitating accurate and timely fault diagnosis (3).

Chapter one provides a general overview of PV systems, their key components,mathematical modeling of the PV system and presents Chapter two we , focuses on classification of common faults and their impact on system performance, providing an overview of the methods of examining faults and how to detect them. Chapter three presents simulation-based analysis using MATLAB/Simulink, where various fault scenarios were introduced and compared with the ideal case. The results demonstrate how early fault detection can significantly enhance system efficiency and reliability.

Chapter 1

Introduction to Photovoltaic Systems and Global Energy Context

1.1 Introduction

The escalating global demand for energy, coupled with pressing environmental considerations and the finite nature of fossil fuel resources, has significantly intensified interest in renewable energy sources. This chapter provides a comprehensive overview of renewable energy, emphasizing its significance, classification, and pivotal role in achieving sustainable energy objectives. The discussion commences with an examination of the limitations and environmental impacts associated with traditional energy systems. Subsequently, a broad introduction to various types of renewable energy is presented.

A particular emphasis is placed on solar energy, attributable to its vast potential and widespread applicability. The latter part of this chapter delves into photovoltaic (PV) technology, introducing critical factors that influence the fundamental operational principles of solar cells, diverse PV technologies, and their respective performance characteristics. This foundational knowledge sets the stage for subsequent chapters, which will explore power losses within PV systems and methodologies for their detection to enhance overall system efficiency.

1.2 Introduction to Energy and the Global Energy Demand

Continuous population growth, ongoing industrialization, and sustained economic development are primary drivers behind the perpetually increasing global energy demand. Historically, traditional energy sources, predominantly fossil fuels, have met the majority of this demand. However, these sources are now confronted with challenges related to depletion and significant environmental impacts(4). The imperative to integrate renewable energy sources stems from the dual need to satisfy this rising demand while concurrently mitigating adverse environmental consequences.

Different segments of the global energy system experienced varied growth rates in 2024, influenced by short-term factors and deep-seated structural trends. Global energy requirements saw an increase of 2.2%, a figure notably higher than the 1.3% annual average observed from 2013 to 2023, partly driven by extreme weather events. Despite

this, energy demand growth was more gradual compared to the global economy, which expanded by 3.2%.

Electricity demand increased by 4.3%, marking the largest absolute increase in several years (excluding immediate post-market recovery periods). This surge was attributed to increased access to power-intensive equipment, a shift towards electricity-based production, digitalization, the proliferation of data centers, advancements in Artificial Intelligence (AI), and growing demand from end-use electrification. The power sector's energy demand was responsible for approximately three-fifths of the total increase.

Regarding energy supply, renewables accounted for a 38% share of the increase in energy generation, followed by natural gas (28%), coal (15%), oil (11%), and nuclear (atomic) energy (8%). The energy intensity of the global economy declined by 1%, and energy-related CO_2 emission growth in 2023 was projected to decrease to 0.8%, below the 1.2% mark.(5)

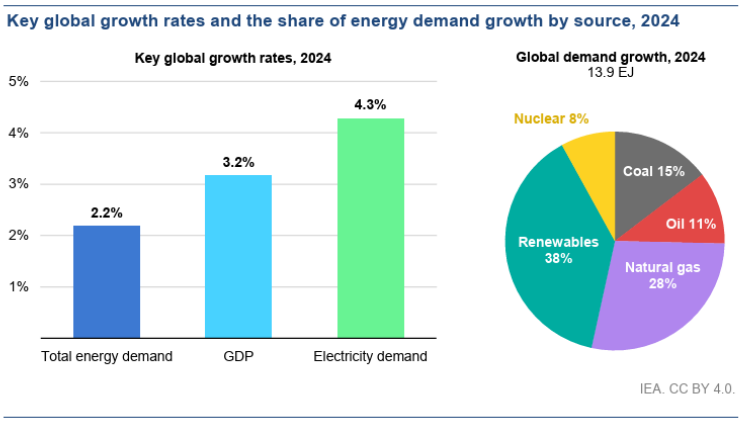

Figure 1.1: Key global growth rates and the share of energy demand growth by source, 2024. (Source: IEA. CC BY 4.0.

1.3 Renewable Energy Sources Classification

Renewable energy sources are derived from natural processes that are continuously replenished, offering sustainable alternatives to conventional fossil fuels. These sources are broadly classified based on their origin and energy conversion methodologies. According to recent data and classifications from prominent organizations such as the International Renewable Energy Agency (IRENA) and the International Energy Agency (IEA), the most significant renewable energy sources include solar, wind, hydroelectric, biomass, and geothermal energy. Each source possesses distinct characteristics and applicability within the global energy landscape (projected for 2025).

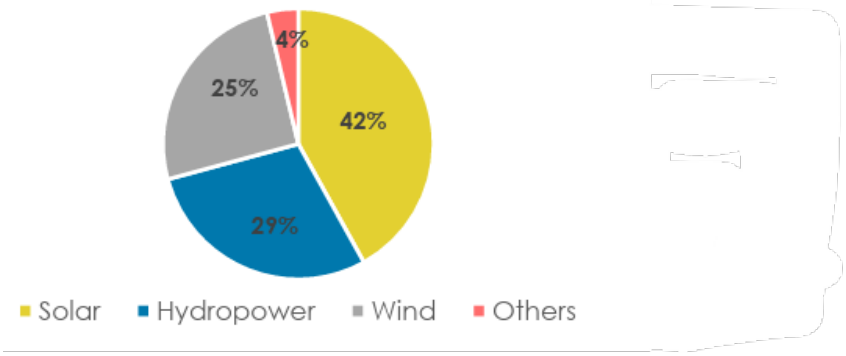

Figure 1.2: Renewable power capacity by energy source

At the end of 2024, global renewable power capacity amounted to 4,448 GW. Solar energy, continuing its trend from the previous year, accounted for the largest share of this total, with a capacity of 1,865 GW. Hydropower and wind energy constituted most of the remainder, with total capacities of 1,283 GW and 1,133 GW, respectively. Other renewable capacities included 151 GW of bioenergy, 15 GW of geothermal energy, and 0.5 GW of marine energy.(6)

1.3.1 Solar Energy

Solar energy harnesses sunlight, utilizing either photovoltaic (PV) cells or solar thermal (solar-heated) technologies. It is an abundant resource, widely accessible globally, and scalable from small residential installations to large utility-scale power plants. PV technology directly converts solar radiation into electricity through the photovoltaic effect in semiconductor materials. Rapid cost reductions and significant technological advancements have positioned solar PV as the fastest-growing renewable energy source, projected to become the largest contributor to global renewable power capacity.(7)

1.3.2 Wind Power

Wind energy involves the conversion of the kinetic energy of wind currents into electrical power using wind turbines. It is a mature and cost-effective technology with substantial deployment in both onshore (coastal) and offshore environments. Wind energy production is anticipated to surpass hydropower by 2030, reflecting its expanding contribution to the overall energy mix.(6)(7)

1.3.3 Geothermal Energy

Geothermal energy originates from the Earth's internal heat, generated by radioactive decay and planetary formation processes. This results in temperatures that can exceed 1000°C at significant depths, with an average geothermal gradient of approximately 0.03°C/m (or 30°C/km). Unlike intermittent renewable sources such as solar and wind, geothermal energy can provide stable, CO_2-free baseload power from virtually inexhaustible reserves. Currently utilized in 26 countries (including the U.S., Indonesia, and Iceland), its economic viability is highest in regions with significant volcanic activity. Modern geothermal plants employ steam-driven or binary cycle systems and are

typically located within 10 km of the resource to minimize thermal losses. Recent technological advancements have markedly improved geothermal energy implementation and performance.(4)

1.3.4 Biomass Energy

Biomass energy is derived from renewable organic materials originating from plants, animals, and microorganisms. It represents stored solar energy captured through photosynthesis. Biomass can be used directly (e.g., combustion for heat) or converted into various forms of energy, such as electricity, heat, and biofuels.(1)

1.3.5 Hydropower

Hydropower utilizes the kinetic or potential energy of flowing or stored water to generate electricity. It is one of the largest and most established renewable energy sources.(6)(7)

1.4 Principle of PV Systems

Photovoltaic (PV) systems operate based on the photovoltaic effect, a physical phenomenon wherein certain semiconductor materials generate an electric current when exposed to sunlight. This principle forms the basis for converting solar energy directly into electrical energy without direct emissions.(8)

Key aspects of PV theory include:

- **Semiconductor Material:** PV cells are primarily composed of semiconductor materials, typically silicon. When sunlight (photons) strikes the cell, it excites electrons within the semiconductor, creating electron-hole pairs.(8)
- **PN-Junction and Electric Field:** The core structure of a PV cell includes a PN-junction, formed by joining p-type and n-type semiconductor materials. This junction creates an internal electric field that separates the light-generated electrons and holes. Electrons are driven towards the n-type layer, while holes move towards the p-type layer, thereby establishing a voltage difference.(8)
- **Electrical Power Generation:** When the PV cell is connected to an external circuit, the separated electrons flow through the circuit, producing a direct current (DC). This current can be used immediately, stored in batteries, or converted to alternating current (AC) using inverters for grid compatibility or to power AC loads.(8)
- **Module and System Formation:** Individual solar cells are electrically connected, typically in series and parallel, to form modules or panels. These modules are then combined into arrays (matrices) to achieve the desired voltage and current levels for various applications, ranging from small residential systems to large-scale solar farms.(8)

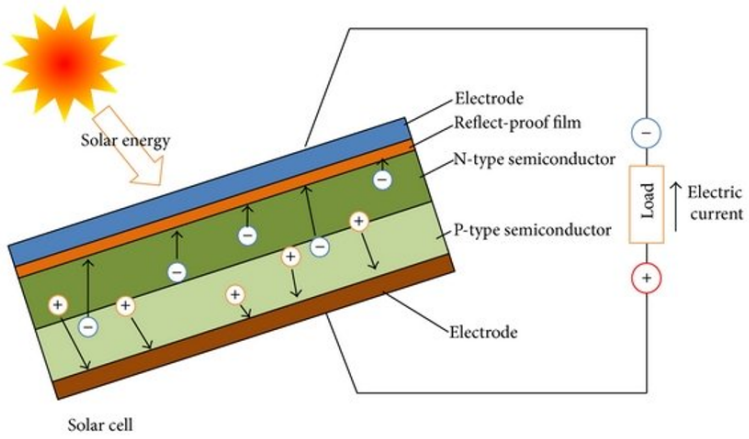

Figure 1.3: Schematic operating principle of a PV solar cell.

1.4.1 Classification of Photovoltaic (PV) Systems

Photovoltaic systems can be classified based on several criteria, including their connection to the electrical grid, application type, system design, and the specific technology employed. The main classifications are as follows:

1. **Grid-Connected (On-Grid) Systems:** These systems are directly connected to the utility grid. When solar energy production exceeds local demand, surplus electricity can be fed back into the grid (net metering/feed-in tariffs). Conversely, when solar generation is insufficient (e.g., at night or during cloudy weather), power is drawn from the grid. They typically include an inverter to convert DC from solar panels to grid-compatible AC. Grid-connected systems are widely adopted due to their cost-effectiveness and ability to reduce electricity bills in residential, commercial, and utility-scale applications.(9)

2. **Stand-Alone (Off-Grid) Systems:** Stand-alone PV systems operate independently of the utility grid. They supply power directly to a dedicated load or, more commonly, charge a battery bank for energy storage. These systems are essential in remote areas without grid access and require robust energy storage solutions to ensure power availability when sunlight is not present.(9)

3. **Hybrid Systems:** Hybrid PV systems combine solar energy with other energy sources, such as diesel generators, wind turbines, or extensive battery storage systems. They offer enhanced reliability and flexibility, particularly in areas with variable solar resources or critical power requirements. The integration of multiple sources and storage can optimize energy use and reduce reliance on any single source.(9)

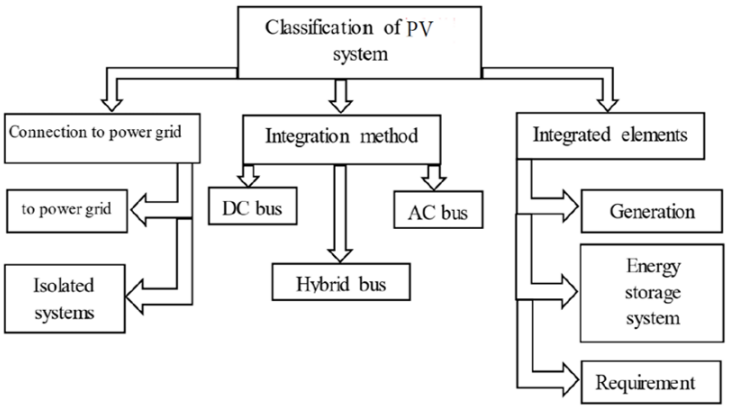

Figure 1.4: Classification of photovoltaic (PV) systems.

1.5 PV Module Modeling

A simplified equivalent circuit model is commonly used to represent a PV cell's electrical behavior. The practical model of a photovoltaic cell incorporates series resistance (R_s) and shunt resistance (R_{sh}) into the ideal diode model, as illustrated in Figure **??**. The single-diode model is often preferred for its simplicity, characterized by a reduced number of equations and parameters compared to the more complex two-diode model, while still providing adequate accuracy for many applications.(10)

The current (I) generated by the PV panel can be expressed as:

$$I = I_L - I_0 \left[\exp\left(\frac{q(V + IR_s)}{nkT} \right) - 1 \right] - \frac{V + IR_s}{R_{sh}} \tag{1.1}$$

where I_L is the light-generated current, I_0 is the diode reverse saturation current, q is the elementary charge (1.602×10^{-19} C), V is the cell output voltage, R_s is the series resistance, n is the diode ideality factor (typically between 1 and 2), k is Boltzmann's constant (1.381×10^{-23} J/K), T is the cell temperature in Kelvin, and R_{sh} is the shunt resistance.

The current flowing through the diode (I_D) is given by:

$$I_D = I_0 \left[\exp\left(\frac{q(V + IR_s)}{nkT} \right) - 1 \right] \tag{1.2}$$

Thus, the output current of the solar cell can also be expressed as:

$$I = I_L - I_D - I_{sh} \tag{1.3}$$

where $I_{sh} = (V + IR_s)/R_{sh}$ is the current through the shunt resistance.

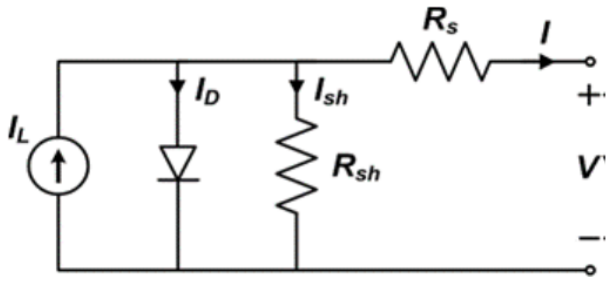

Figure 1.5: The electrical equivalent circuit model of a single-diode PV cell.

The solar cell's output current (I) is dependent on various factors, including I_0, R_s, q, k, T, I_L, V, and R_{sh}. This study examines the SPR-305E-WHT-D solar panel and its performance under Standard Test Conditions (STC: 25 °C cell temperature, 1 kW/m^2 irradiance, Air Mass 1.5 spectrum). The key characteristics are shown in Table 1.1. The Photovoltaic module's Power-Voltage (P-V) and Current-Voltage (I-V) characteristics were measured at various irradiance levels and 25 °C, as illustrated in Figure 1.6.

Table 1.1: Characteristics of the SunPower SPR-305-WHT PV module.

Parameter	Value
Maximum power (P_{max})	305.226 W
Current at MPP (I_{mp})	5.58 A
Voltage at MPP (V_{mp})	54.7 V
Short circuit current (I_{sc})	5.96 A
Open circuit voltage (V_{oc})	64.2 V
Number of parallel strings	66
Series-connected modules per string	5

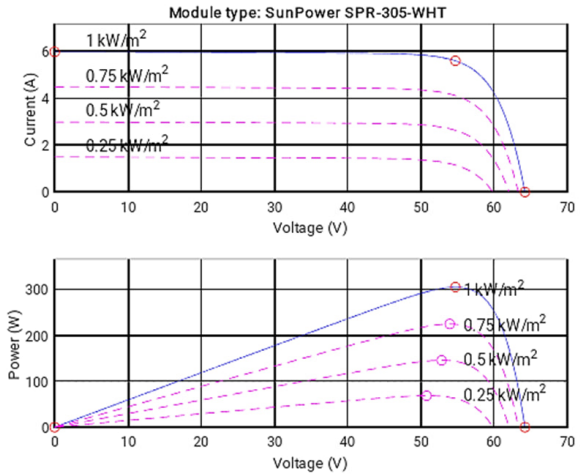

Figure 1.6: The P-V and I-V photovoltaic module's characteristics measured at 25 ∘C and different levels of irradiance.(10)

1.6 Power Converters

Power converters are electronic devices that transform electrical energy from one form to another, such as converting alternating current (AC) to direct current (DC), DC to AC, or adjusting DC voltage levels. They are integral to modern technology, found in applications ranging from mobile phone chargers to large-scale renewable energy systems(11). Power converters typically employ semiconductor switches (like MOSFETs or IGBTs) and passive components (inductors, capacitors) to store and transfer energy. Pulse-Width Modulation (PWM) is a common control technique used to regulate the output, ensuring high efficiency. Converter design must consider factors such as thermal management and electromagnetic interference (EMI) to ensure reliable operation. This research focuses on two fundamental DC-DC converter types: the boost converter and the buck converter, with a particular emphasis on the boost converter for elevating solar panel voltage to meet load requirements.

1.6.1 Boost Converter

The boost converter is a fundamental type of DC-DC converter that increases an input DC voltage to a higher output DC voltage. It achieves this by varying the duty cycle (α) of a control switch, typically between 0 and 1. The relationship between the input voltage (V_{in}), output voltage (V_{out}), and duty cycle is given by(10):

$$V_{out} = \frac{1}{1-\alpha} V_{in} \tag{1.4}$$

where V_{in} is the voltage supplied to the input of the converter, V_{out} is the voltage supplied at the output of the converter, and α is the duty cycle of the switch 'S' (see Figure **??**). A DC-DC boost converter is often used in PV systems to step up the panel voltage for battery charging or grid connection, and it plays a crucial role in Maximum Power Point Tracking (MPPT) by adjusting the effective load seen by the PV panel.

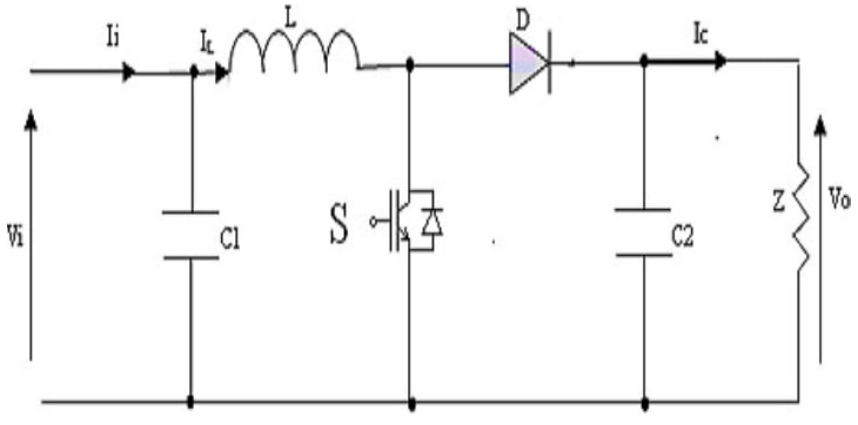

Figure 1.7: Electrical configuration of the boost power converter.

1.6.2 Buck Converter

A buck converter is a DC-DC converter that steps down an input DC voltage to a lower output DC voltage. This is vital in PV systems where solar panels produce a variable

voltage (dependent on sunlight) that might be too high for charging batteries or powering certain devices directly. Buck converters provide a stable, lower voltage output, enhancing system efficiency and reliability. The primary function is to decrease voltage while (ideally) increasing current capability, conserving power. The output voltage (V_{out}) is related to the input voltage (V_{in}, denoted as V_{int} in the original text) and the duty cycle (D) by equation (1.5).

$$V_{out} = V_{in} \cdot D \tag{1.5}$$

The duty cycle D is defined as:

$$D = \frac{T_{on}}{T_{on} + T_{off}} = \frac{T_{on}}{T_s} \tag{1.6}$$

where T_{on} is the time the switch is closed, T_{off} is the time the switch is open, and $T_s = T_{on} + T_{off}$ is the switching period (Figure **??**).

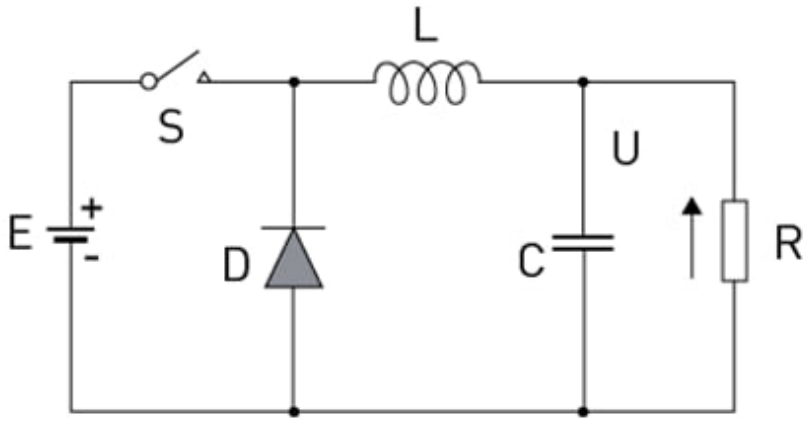

Figure 1.8: The Buck Converter Circuit Diagram.

1.7 Maximum Power Point Tracking (MPPT) Techniques

The output power of a PV panel is highly dependent on solar irradiance and cell temperature, resulting in a non-linear I-V characteristic with a unique Maximum Power Point (MPP). MPPT techniques are algorithms implemented in power converters (typically DC-DC converters) to continuously adjust the operating point of the PV array to ensure it operates at or near this MPP, thereby maximizing the energy harvested.

1.7.1 Perturb and Observe (P / O) Method

The Perturb and Observe (P&O) method is a widely adopted MPPT algorithm in PV systems due to its simplicity and ease of implementation. The technique operates by periodically perturbing (i.e., slightly increasing or decreasing) the PV array's operating voltage or the duty cycle of the associated converter, and then observing the resulting change in power output. If the power increases, the perturbation continues in the same direction; otherwise, it is reversed.(12)

However, P/O can suffer from oscillations around the MPP under steady-state conditions, leading to some power loss(13). It may also struggle to track the MPP accurately during rapid changes in irradiance. To mitigate these drawbacks, adaptive step-size P&O variants and other advanced algorithms have been proposed, improving tracking speed and accuracy under dynamic weather conditions(14). Despite its limitations, P&O remains popular in commercial PV systems, particularly due to its low computational cost and minimal hardware requirements.(15) Figure **??** illustrates the flowchart for the P&O method.

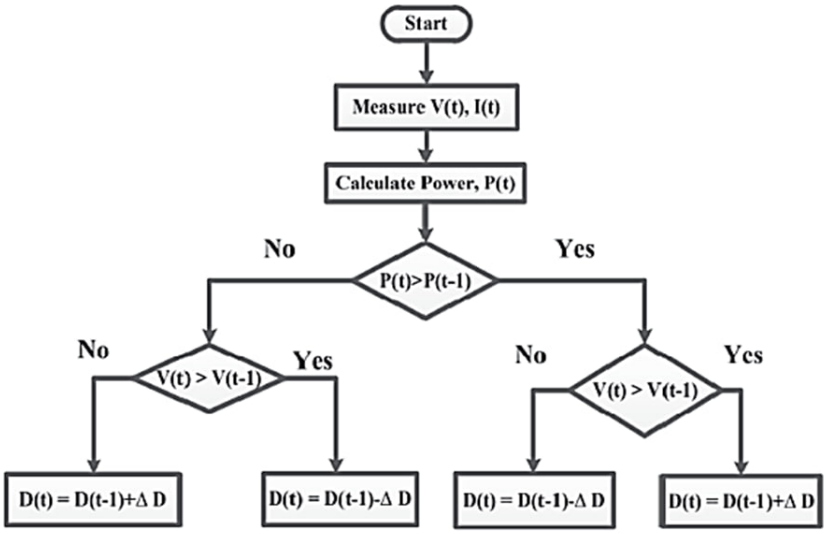

Figure 1.9: Flowchart for P & O method.

1.8 Inverters

Inverters are a critical interface in PV systems, responsible for converting the variable direct current (DC) output from solar panels into grid-compatible alternating current (AC)(16). Modern inverters often include MPPT algorithms, such as P&O or Incremental Conductance,(17) to optimize energy harvesting under varying environmental conditions. Advanced Multilevel Inverter (MLI) topologies, including Neutral-Point Clamp (NPC) and Cascaded H-Bridge (CHB) designs, have demonstrated superior performance by reducing Total Harmonic Distortion (THD) and improving overall system efficiency.(18)

Furthermore, smart inverter technologies now provide essential grid-support functions. These include reactive power control (e.g., PV-STATCOM functionality for voltage regulation) and Fault Ride-Through (FRT) capabilities, enabling the PV system to remain connected and support the grid during transient disturbances, even during periods of non-generation(19). Current research often focuses on hybrid MPPT techniques that combine traditional algorithms with metaheuristic approaches to address challenges like partial shading, achieving tracking efficiencies exceeding 98% (20). These technological advancements have made modern inverters indispensable for both small-scale residential and large-scale utility PV installations.(21)

1.9 Grid-Connected Photovoltaic Systems

Grid-connected photovoltaic (PV) systems require sophisticated synchronization mechanisms to maintain power quality and stability when interfacing with utility grids.(22) These systems employ grid-tied inverters that must adhere to strict standards and grid codes (e.g., IEEE 1547 in North America, EN 50549 in Europe) concerning voltage regulation, frequency stability, and protection schemes, including anti-islanding (23). Anti-islanding protection ensures that the PV system ceases to export power to the grid when the grid itself experiences an outage, preventing safety hazards for utility workers and potential damage to equipment.(24)

Modern smart PV inverters offer supportive ancillary services, such as reactive power support (Volt-Var control) and ramp-rate control, to mitigate voltage fluctuations arising from the intermittency of solar generation(25). However, high penetration levels of PV systems, especially in weak distribution networks, can raise concerns regarding reverse power flow and voltage rise issues (26). Advanced solutions, including adaptive Volt-Var control strategies and Distributed Energy Resource Management Systems (DERMS), have proven effective in maintaining grid stability even with PV penetration levels exceeding 30% (25). These developments are crucial for facilitating the transition towards renewable-dominated power systems while ensuring continued grid reliability and security.(27)

Chapter 2

Classification of PV System Faults

2.1 Introduction

The Photovoltaic (PV) system has proven to be an important technique in global change to permanent energy, due to their modularity, low environmental footprints and rapid reducing costs. Still, these systems are not immune to errors - whether it is mechanical, electric, thermal or environment - which can reduce their performance and lifetime. Identifying and understanding such errors is important for many interconnected reasons. First, even small defects can cause uneven drops in microscopic cracks in cells or loose electrical contact electricity production. Over time, these disadvantages, the total system, reduce efficiency and reduce the expected energy yield. Secondly, uncontrolled incorrect system reliability: Intermittent errors or unplanned shutdowns not only disappoint end users, but also complicate web integration, especially for large PV installations.

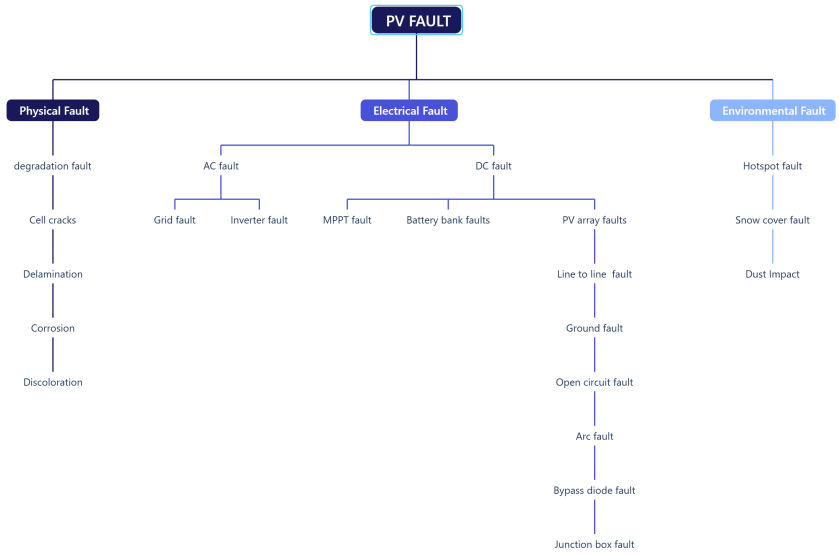

Figure 2.1: Classification of PV System Faults

The diagram illustrates Figure 2.1 the faults in a solar PV system fall into three buckets: physical, electrical, and environmental. Physical faults are the kinds of wear-and-tear you'd expect things like cracked cells, layers peeling apart, corrosion, or the panels simply changing color over time from stress or manufacturing quirks. Electrical faults break down into AC-side issues (for example, problems with the grid connection or

the inverter) and DC-side issues, which cover everything from an MPPT tracker glitch to battery-bank failures and a host of array-level faults ground faults, open circuits, arc faults, bypass-diode failures, right down to a misbehaving junction box. Finally, environmental faults come from Mother Nature: hot spots, snow piling up, even dust settling on the panels can reduce performance or trigger a fault. In practice, understanding where a problem sits in this tree helps technicians pinpoint and fix it much faster.

2.2 Mechanical Faults

most flaws in solar panels things like encapsulation problems, corrosion, microcracks, and general wear come down to mechanical stress or the materials used when they're made. Picking tougher, corrosion-resistant stuff can really stretch a panel's lifespan and cut down on breakdowns.(28) Here's what happens when cells start degrading: their output current drops, and they can even lose color intensity. This wear and tear ramps up internal resistance, tanks efficiency, and can wreck the anti-reflective coating that grabs sunlight. Bottom line These issues can slash a panel's power output to nearly half of what it should be.(29)

2.2.1 Cell cracks

As seen in Figure 2.2, cell cracks are fractures that have formed in the silicon substrate of the PV module. In addition to the silicon substrate, fractures may also develop in the various lamination layers of the cell. When these cracks also referred to as microcracks become too tiny for the human eye to discern, electroluminescence imaging can be used to identify them. Several primary causes of cracks are mentioned in (30) and include: mechanical stress during production, transportation, or installation; potential shocks during transportation; manufacturing improper handling during packaging aging of cells high temperatures and hailstorms snow cover, wind, and rain.

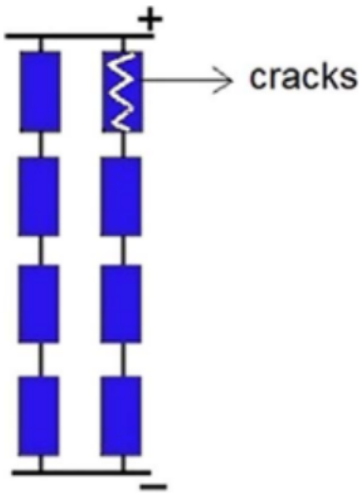

Figure 2.2: Crack in solar PV panel

2.2.2 Delamination

When layers in a solar module don't bond properly – whether between the glass, encapsulant, solar cell, or back sheet – gaps or peeling occur. This delamination like Figure 2.3 causes sunlight to bounce off instead of getting absorbed, while also letting moisture or air sneak into the gaps. These issues often snowball into other failures. Ultimately, peeling or discoloration in a PV module signals encapsulation failure, usually triggered by moisture intrusion, salt buildup, or environmental wear and tear.(30)

Figure 2.3: delamination of solar panel

2.2.3 Corrosion

humidity can seep into solar panels when protective layers delaminate or develop cracks, leading to material corrosion. This especially affects the delicate silver grid lines on cell surfaces and their metal base connections, which corrode when exposed to common atmospheric gases like carbon dioxide, sulfur, and oxygen . As shown in Figure 2.4, this corrosion visibly damages panel components. The consequences are twofold: corroded wiring increases electrical resistance causing significant power losses, while deteriorated metal contacts may create dangerous leakage pathways through the system (31).

Figure 2.4: corrosion in solar cell (35)

2.2.4 Discoloration

You can often spot solar cell discoloration just by looking at the panels what should appear white gradually turns yellow or brown Figure 2.5 . This color change actually blocks sunlight from reaching the cells properly. Less light absorption means more heat builds up, which significantly reduces the system's power output over time. Several factors cause this yellowing effect, including prolonged exposure to UV rays, thermal stress from temperature swings, trapped gases or acids between material layers, and even corrosion creeping into the metal connections (32).

Figure 2.5: Discoloration of solar cell

2.3 Electrical Faults

Photovoltaic (PV) systems are important for using renewable energy, converting solar energy to electricity. However, electrical defects can reduce efficiency, accelerate aging and reduce the security risk, among the most important and influential of these faults is the electrical fault. (33)

2.3.1 AC faults

AC faults typically happen on the alternating current side of solar installations specifically in the inverter or where the system connects to the grid. These electrical issues are critical because they can shut down power delivery even when panels are generating electricity. In the next section, we'll examine common inverter and grid connection problems that fall under this AC fault category.(33)

2.3.1.1 Grid fault

In grid-connected solar systems, the PV array feeds power through an inverter that parallels the utility grid or distribution . During grid outages, this connection must immediately disconnect through anti-islanding protection preventing any solar-generated electricity from backfeeding into the de-energized grid . Common grid-side faults include transmission line damage, substation failures, blackouts, overloading conditions, and weak connections that compromise power quality(34).

2.3.1.2 Inverter fault

Solar panels produce direct current (DC). It flows into the DC power inverter, which converts it into an alternative current (AC) required for your home or grid. Unfortunately, inverters often fail because of a few key problems: sloppy installation, unstable voltage or current, or simply being overloaded by demanding appliances (35). Safety is critical here. If the main power grid goes down, inverters connected to it must quickly disconnect the solar system. If they don't manage this cutoff properly, it could put utility repair crews in serious danger.

2.3.2 DC faults

Its about the DC part on the system including PV array, battery bank, and maximum power point tracker (MPPT) failures.

2.3.2.1 MPPT fault

Solar panels work at their best when delivering power to the inverter, thanks to the Maximum Power Point Tracker (MPPT). Essentially, it's an algorithm built into the charge controller that squeezes the most possible energy out of the panels, especially when sunlight or temperature changes. But if the controller itself is faulty, the MPPT might not do its job right. When that happens, you'd see the system's output voltage and overall power take a noticeable drop (34).

2.3.2.2 Battery bank faults

Solar cells produce electric current when sunlight hits them. But when there's no sun, battery banks take over to keep the power flowing steadily. These batteries connect to the solar panel system. They charge up during the day and then run your devices at night. things often go wrong Charging. Irregular charging patterns are usually to blame when these batteries fail unexpectedly.(35)

2.3.2.3 PV array faults

The seven types of PV array faults which are discussed in the following section are: Earth fault, Line-to-Line fault, Bridging fault, Open circuit fault, Arc fault, Bypass diode fault and Junction box fault.(34)

- `LINE TO LINE FAULT`:A line-to-line fault in a solar array like in Figure 2.6 happens when cables or connections at different voltages accidentally short together. This can occur in two distinct ways: Within a single string (intra-string fault) Between adjacent strings (cross-string fault) The immediate consequence a sudden voltage drop across the system – which clearly shows up as a distortion in its voltage-current (VI) curve (36) .

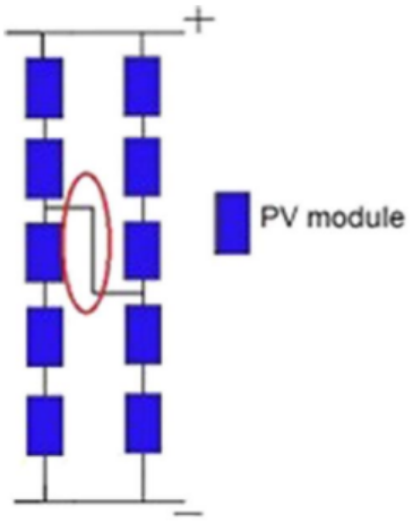

Figure 2.6: Line to line fault

- `short circuit ( ground fault )`:A ground fault (or earth fault), shown in Figure 2.7, is a type of short circuit that creates an accidental path for current to flow into the earth , Metal parts that shouldn't carry current are connected to earth grounded for safety. This protects people from electric shock if something goes wrong, If a live conductor accidentally touches this grounded metal, a sudden surge of current flows through the metal and straight into the ground ,In PV arrays, this surge creates a "mismatch fault" through the grounded parts. Ground faults fall into two main types: lower earth faults and upper earth faults.(37)(36)

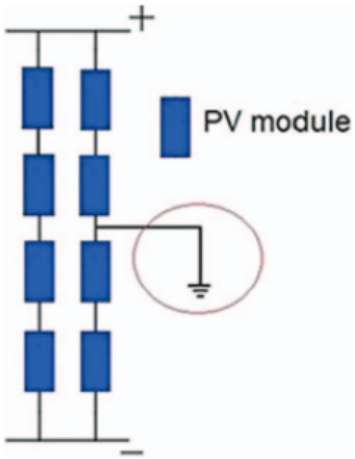

Figure 2.7: Short circuit between the PV module and the ground.

- `Open circuit fault`:An open circuit defect happens when the wire carrying current to your load gets cut or disconnected. This usually stems from incorrect wiring or loose connections between system components. See Figure 2.8 for an example in a solar panel setup. Here's the catch: as more panels or strings disconnect,

you'll see a clear drop in both short-circuit current and maximum power output. Surprisingly though, the system voltage stays almost normal (36).

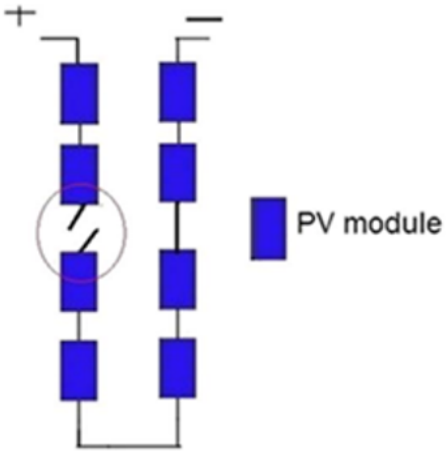

Figure 2.8: Open circuit fault

- `Arc faults` : Arc faults often start with flimsy connections in the circuitry especially where components join in series or parallel. cold solder joints, loose terminals, or cracked insulation. Here's the real danger: Arcs generate extreme heat. If this superheated plasma touches flammable materials? You get fire. That's why these faults are such a serious fire hazard – the plasma discharge literally ignites surrounding materials ,there are two types of arc faults Series Arcs Parallel Arcs . Parallel arcs pull massive current surges because they short-circuit high-voltage points. Series arcs draw less current but are still dangerously (38).

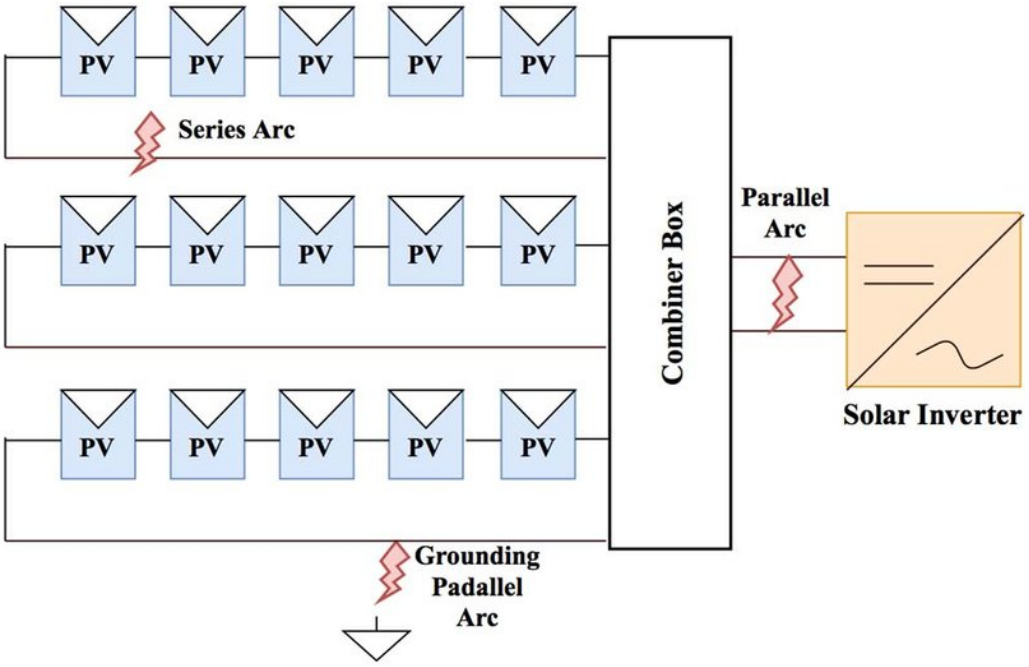

Figure 2.9: series and parallel arc faults

- `Bypass diode fault`:Bypass diodes connect across groups of cells in solar panels like an insurance policy. Normally (with no shading), they sit idle. But during partial shading, shaded cells can overheat by resisting current flow instead of generating power. That's where bypass diodes kick in – they give the current an alternative path around the struggling cells, preventing dangerous heat buildup (39). If a defective bypass diode is installed, it becomes the problem. Instead of protecting the panel, a faulty diode can create hotspots under shading by blocking current when it shouldn't. This trapped heat can literally melt components or ignite fires (40). The very component meant to solve overheating (the bypass diode) can cause catastrophic failure if it's damaged or low-quality (39), (40).

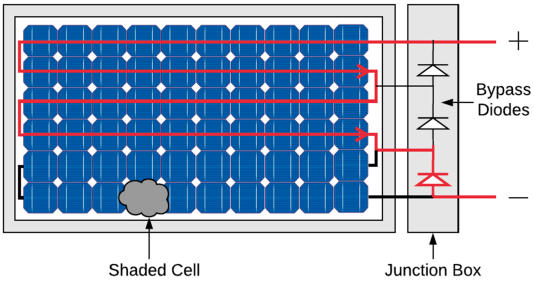

(a) PV module with one shaded cell(41)

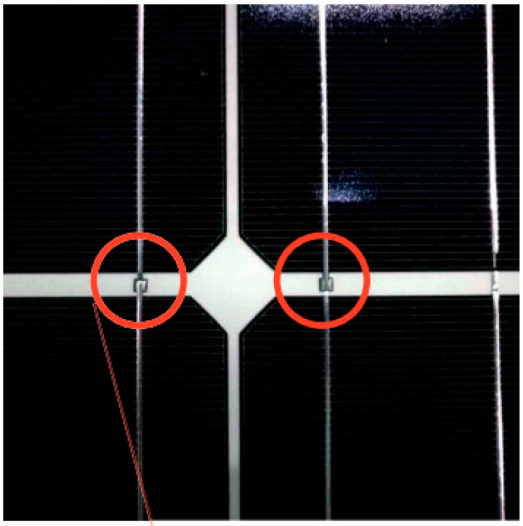

(b) . BP diodes place on each cell (42)

Figure 2.10: BP diodes

- `Junction box failure`:Junction box Figure 17 reliability is make-or-break for any field-deployed PV system. Industry studies reveal 85% of failures originate during installation (poor workmanship, field repairs), while 15% stem from manufacturing defects (41).

Figure 2.11: The faulty examples for rework cable of junction box (43)

2.4 Environmental Fault

Solar arrays face constant stress from their environment. Weather shifts, varying sunlight, partial shading, temperature extremes, and other factors directly impact performance and can cause serious – sometimes permanent – damage to PV cells. This section explores these environmental failure modes in detail.(32)

2.4.1 Hotspot fault

Hotspot faults represent a critical temperature-related failure in PV panels, creating dangerous localized "heat islands" significantly hotter than surrounding areas. These zones exhibit abnormal electrical behavior (visible in IV curves) and stem primarily from defective cells or partial shading. The core issue occurs when current mismatches – caused by uneven power flow from input to output – force operating current to exceed a shaded defective cell's reduced short-circuit capacity, igniting intense localized heating. Severity escalates with both the degree of electrical mismatch and its duration. Common triggers include panel aging, surface debris accumulation (dust, soil, bird droppings), snow cover, and other soiling agents – all capable of degrading performance and accelerating permanent damage through sustained hotspots (36).

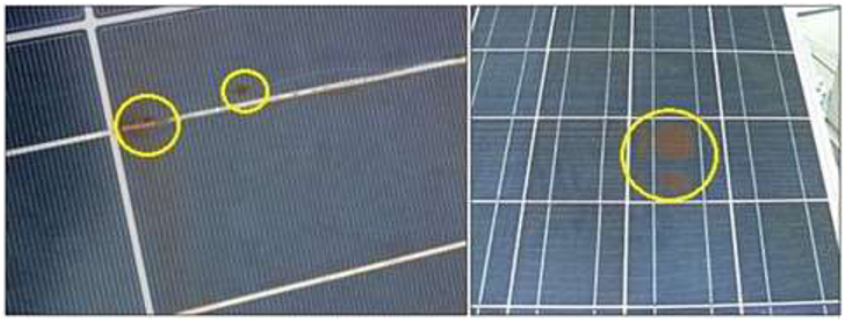

Figure 2.12: Damaged cells due to hotspot fault [41]

2.4.2 Snow cover

Snow accumulation on solar panels during winter creates immediate trouble the covered cells become partially shaded, triggering mismatch faults. This shading throws off the panel's electrical behavior (IV characteristics), causing localized temperature spikes that ignite hotspots. Over time, these hotspots accelerate wear while the snow itself physically degrades the panel's surface properties (26), (25). You can see this snow-induced shading effect visually in Figure 2.13 – a silent but damaging winter threat to PV performance.

Figure 2.13: Solar PV panel full covered and partially covered by snow

2.4.3 Partial shading fault

Partial shading occurs when even a small section of a solar panel is covered, instantly cutting the system's power output. The shaded cells can't generate electricity – instead, they heat up like resistors and trigger dangerous hotspots. These hotspots silently damage panels over time. Common culprits include bird droppings, nearby buildings or trees, fallen leaves, passing clouds, snow cover, dust buildup, and uneven sunlight distribution (36) . (42). You can see real-world examples of this shading effect in Figure 2.14.

Figure 2.14: Partial shading

2.4.4 Dust impact

Dust is a stealthy thief of solar efficiency. When fine particles settle on panel surfaces, they create a hazy barrier that scatters and blocks sunlight – technically called soiling loss. This directly slashes power output, sometimes by 20% or more in arid regions (43). Unlike sudden shading, dust accumulates gradually, making its impact easy to overlook. Critically, uneven dust patterns create partial shading effects, forcing unsoiled cells to overcompensate and triggering dangerous hotspots. Left unchecked, this grimy layer doesn't just reduce daily yield; it accelerates long-term wear. Regular cleaning is essential, especially in dusty environments where residue becomes cement-like after rain. Visual examples of dust shading appear in Figure 2.15.

Figure 2.15: Dust impact on solar panel

2.5 Photovoltaic Fault Detection Methods

Photovoltaic fault detection and diagnosis methods are categorized into three core methodologies: **Process-History Based**, **Quantitative-Model Based**, and **Signal-Processing Based** approaches. These techniques leverage critical system measurements to identify failures(29), including:

- **Environmental parameters:** Solar irradiance (G) and module temperature (T)
- **DC-side characteristics:** Maximum power point coordinates (MPPT) and full I–V curve
- **AC-side outputs:** Inverter voltage (V_{AC}) and current (I_{AC})

By analyzing these data streams, each method provides unique diagnostic capabilities across the PV system's operational spectrum.(36)

2.5.1 Process-History Based Methods

Process-History Based Methods leverage historical operational data to detect irregularity through statistical analysis and machine learning. These techniques identify deviations from expected performance patterns by analyzing long-term datasets, including energy yield records, maintenance logs, and Supervisory Control and Data Acquisition (SCADA) system outputs. Key measurements include solar irradiance (G) and module temperature (T), which contextualize power fluctuations. For instance, auto-regressive models or neural networks correlate performance degradation with environmental stressors, enabling early detection of faults like delamination or potential-induced degradation (44). While cost-effective for large-scale installations due to minimal hardware requirements, these methods lack granularity in pinpointing fault locations and may miss transient failures (45).

2.5.2 Quantitative-Model Based Methods

Quantitative-Model Based Methods employ physics-based simulations to compare real-time system behavior against theoretical models. These approaches utilize equivalent circuit models (e.g., single-/double-diode models) to simulate ideal current–voltage (I–V) characteristics under given irradiance (G) and temperature (T) conditions. Faults manifest as disparities between measured parameters—such as maximum power point coordinates I_{AC}, V_{AC}, and model predictions(46). For example, line-to-line faults reduce V_{mpp} by more than 15% relative to simulated values, while bypass diode failures distort the I–V curve's inflection points (47). Though highly accurate for DC-side faults, computational complexity and model sensitivity to parameter drift remain limitations (48).

2.5.3 Signal-Processing Based Methods

Signal-Processing Based Methods extract fault signatures from electrical waveforms using transformation techniques. Time-domain or frequency-domain analyses (e.g., wavelet transforms, Fourier analysis) decompose inverter output signals (I_{AC}, V_{AC}) or I–V sweeps to isolate irregularity. Arc faults generate high-frequency harmonics (>100 kHz), detectable via discrete wavelet coefficients (49), while partial shading induces step-changes in dV/dI profiles (47). Real-time implementations use field-programmable gate arrays (FPGAs) for rapid fault classification but require high sampling rates (>200 kS/s) and noise filtering (50). This approach excels in diagnosing transient AC-side faults but struggles with slow-evolving degradation.

2.6 Conclusion

Solar panels are getting more and more important for powering our world, so we've got to make sure they keep working well for a long time. This chapter digs into the main problems that can mess them up, like when the cells crack or the layers start peeling apart, issues with the electrical stuff—whether it's in the panels or the grid connection—and things like dust, snow, or shade getting in the way.

Each of these hiccups can cause its own kind of trouble. Cracks or peeling might slowly cut down how much energy the panels put out, but electrical glitches or a bunch of snow can stop things cold, sometimes out of nowhere. Figuring out what causes these issues and how they play out helps us build tougher systems and fix stuff before it turns into a bigger headache.

The chapter also gets into some new ways to spot these problems early like using data from how the system's been running, science-based models, These diagnostic tools facilitate the early detection of potential faults, enabling proactive maintenance and ensuring the seamless operation of photovoltaic systems while mitigating the risk of significant disruptions.

Chapter 3

Simulation results and discussions

3.1 Introduction

In this chapter, we present the simulation work done to study how a 100 kW grid-connected photovoltaic system behaves under different conditions we start by explaining how the system works under ideal conditions, then introduce faults at various points, including the PV array, converter, and grid, for each case, we examine the effects on voltage, current, and power, helping us understand how different failures impact the overall system. Our object is to detect photovoltaic systems Fault based on power losses analysis based on systeme output and compare it with the system output in the optimal case , a simuluation was conducted using Matlab/Simulink environment

3.2 Simulink Model of the System

The global control schema block for the 100-kW grid-connected photovoltaic (PV) array system integrates several essential elements to control the system's operation effectively. It includes an "inputs" block that provides the reference signals, such as desired power output or grid synchronization requirements. The "PV Array" block models the photovoltaic generation unit, supplying current and voltage measurements. A "Controller" block, encompassing the boost converter with MPPT and the VSC control, regulates the system's behavior to maximize power extraction and ensure proper grid integration. Additionally, an "Error Calculation" block computes the disparity between the reference values and the actual system measurements, enabling precise control adjustments. The comprehensive block diagram is shown in Figure 3.1.

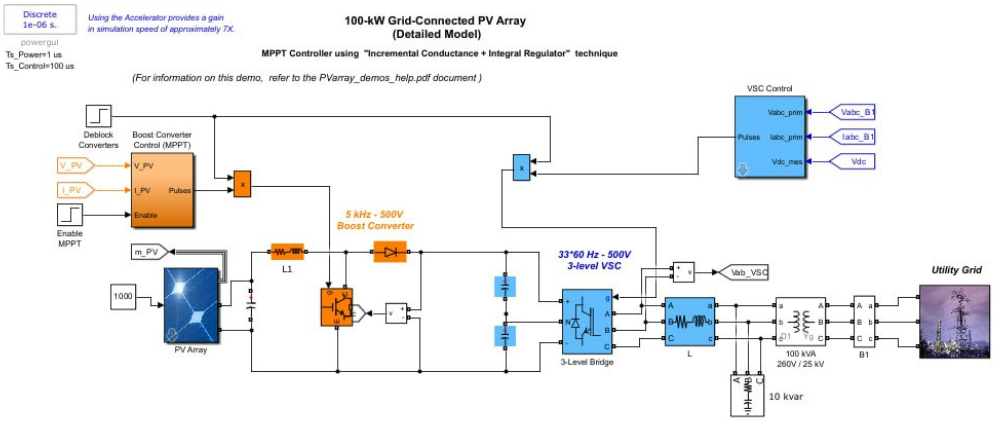

Figure 3.1: Global Schema Block of a grid-connected PV system (optimal case)

We created errors in the simulation and compared its output with the optimal case, and the errors were at the level of pv array , boost converter and grid .

3.2.1 pv array block

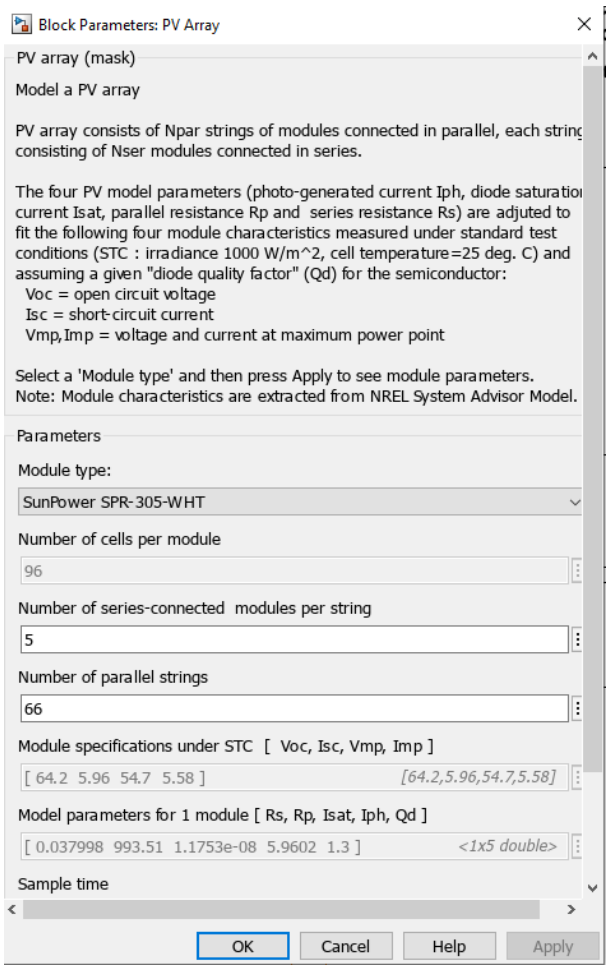

Figure 3.2: Pv array setting

The photovoltaic array used in this study was modeled in Matlab/Simulink to replicate the behavior of a real-world solar power system. The configuration consists of 5 panels connected in series per string, with a total of 66 strings in parallel, yielding a complete array of 330 SunPower SPR-305-WHT modules.

Under standard test conditions (STC), each panel delivers an open-circuit voltage of 64.2 V and a short-circuit current of 5.96 A. The maximum power point is reached at a voltage of 54.7 V and a current of 5.58 A. The model also includes detailed electrical parameters: a series resistance of 0.037998 Ω, a parallel resistance of 993.51 Ω, a saturation current of 1.1753×10^{-8} A, and a diode ideality factor of 5.9602.

This setup enables the analysis of system performance under faulty conditions—such as the disconnection of a string or variations in irradiance—and allows comparison against ideal operation throughout the study.

3.2.2 Boost converter block

The diagram Figure 3.3 boost converter circuit operating at 5 kHz with a 500 V output, a crucial part of the photovoltaic system. It starts with an inductor (L1), which stores energy from the input voltage, followed by a switch and a diode that manage the energy flow. The output is stabilized by capacitors, delivering a steady DC voltage (Vdc) to the load. According to the L1 block parameters, the inductor has a resistance of 0.005 Ohms and an inductance of 5e-3 H, helping to control the current effectively. The C1 block parameters indicate a capacitance of 1200e-06 F, which smooths out the voltage output.

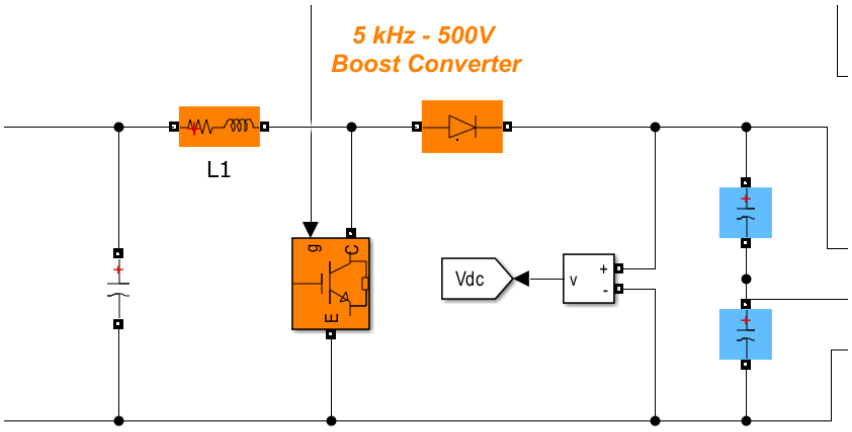

Figure 3.3: Boost converter block

3.2.3 MPPT controller

The Maximum Power Point Tracking (MPPT) controller is designed using the incremental conductance method combined with an integral regulator to optimize the power output of the photovoltaic (PV) system. It operates by calculating the power, $P = V \times I$, and its derivative with respect to voltage, $\frac{dP}{dV}$, to locate the maximum power point where $\frac{dP}{dV} = 0$, which corresponds to the condition $\frac{dI}{dV} = -\frac{I}{V}$.

The controller receives current (I_{PV}) and voltage (V_{PV}) inputs from the PV array, processes them through a series of blocks to compute $\frac{dI}{dV}$ and the associated error, and

then adjusts the duty cycle using an integrator with gain (K_i) to minimize this error. In practical terms, this configuration enables the PV system to dynamically respond to environmental changes—such as fluctuations in solar irradiance—ensuring maximum power extraction. Additionally, the controller includes an "I_V MPPT on/off" switch, allowing manual activation or deactivation of the tracking function.

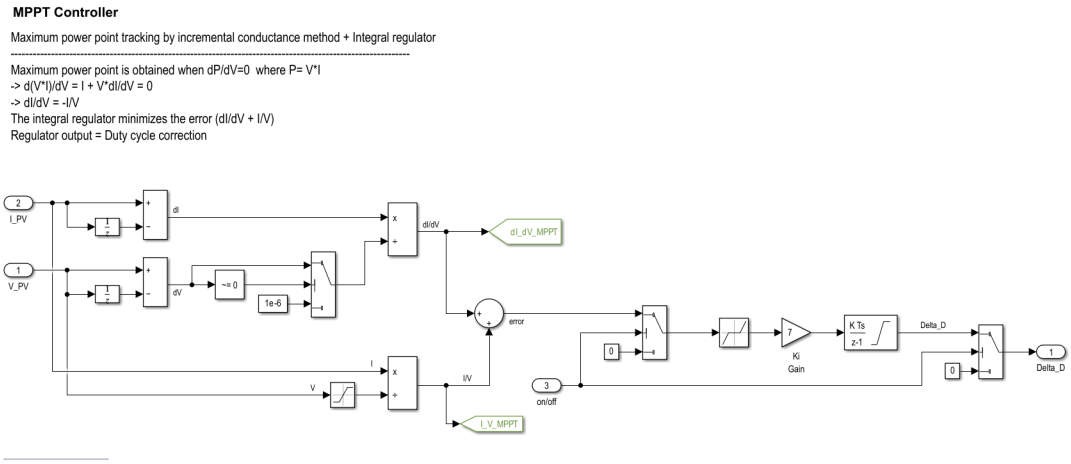

Figure 3.4: MPPT controller

3.2.4 Voltage Source Converter (VSC)

The control system is based on a Voltage Source Converter (VSC) using an average model configuration. At its core is the `VSC Control1` block, which processes several inputs: the reference voltage (U_{ref}), the measured DC voltage ($V_{\text{dc\_mes}}$), and derived signals such as V_{abc_prim} and I_{abc_prim}. These inputs are used to generate outputs: V_{abc_B1} and I_{abc_B1} for the AC side, and V_{dc} for the DC link.

The `VSC (Average Model)` block takes U_{ref} as an input and connects to a three-phase system with terminals labeled A, B, and C. This system is coupled to an inductance component (L), which links to the output lines a, b, and c, forming the interface with the external grid or load.

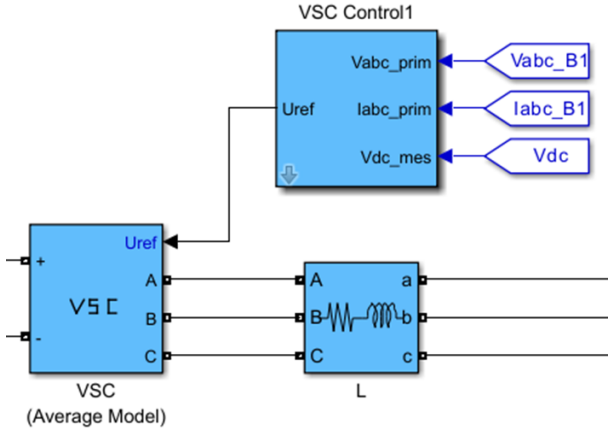

Figure 3.5: The three-level VSC

3.2.5 Utility Grid

The grid-connected simulation setup features a 100 kVA, 260V/25 kV transformer that interfaces a three-phase system (A, B, C) with the utility grid. This configuration includes a 10 kVAr reactive component and appropriate grounding. It incorporates two feeders, one 5 km and the other 14 km in length, connected to a combined load of 30 MW and 2 MVAr.

To reflect realistic grid conditions, the system integrates transformers rated at 47 MVA (120 kV/25 kV) and a high-voltage transformer rated at 120 kV, 2500 MVA. The network terminates with a 3-ohm resistive load. This comprehensive setup is designed to simulate the dynamics of grid-connected power systems, including aspects of power transmission, voltage transformation, and load behavior.

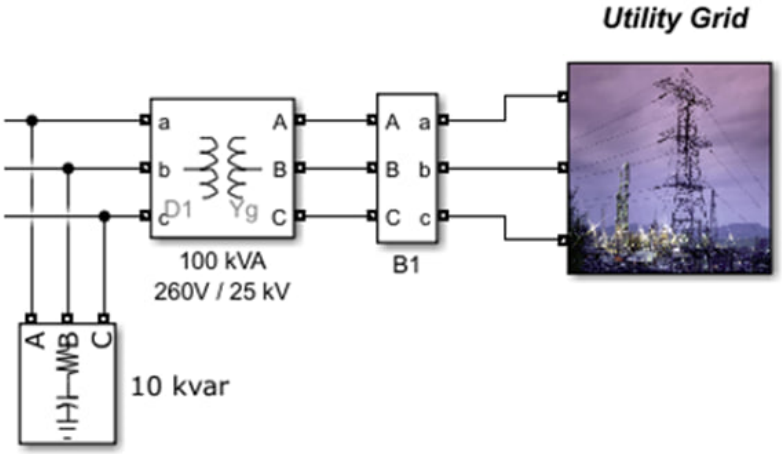

Figure 3.6: Utility Grid

3.3 Testing and results

3.3.1 PV array

3.3.1.1 String down

The first fault analyzed was introduced at the PV array level. Under normal operating conditions, the array consisted of 5 strings with 66 panels each, totaling 330 panels, providing maximum power output. To simulate the fault, one complete string was removed, reducing the configuration to 4 strings (264 panels).

This modification resulted in a noticeable decrease in both current and voltage, which in turn caused a drop in the overall power output. The scenario represents a practical fault condition, such as the disconnection of a string due to wiring issues, panel malfunction, or maintenance requirements. The simulation underscores the proportional relationship between array capacity and power generation, illustrating the significant impact of string-level faults on system performance.

- results at pv arry level

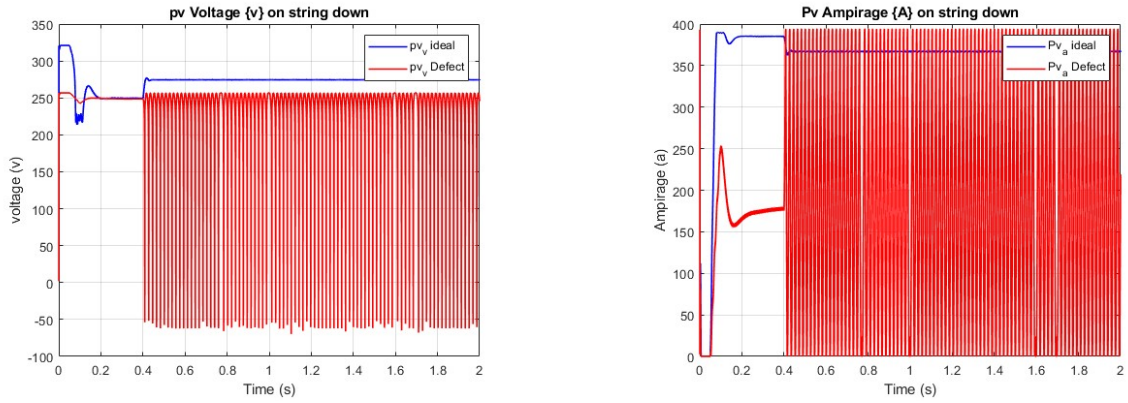

(a) PV voltage

(b) PV amperage

Figure 3.7: PV arry results at string down

The voltage and current output curves for the PV array highlight the impact of the simulated fault. For the voltage (V_{PV}), the optimal case shows a stable value around 280 V after an initial transient, while under fault conditions, it drops to approximately 200–250 V, with noticeable oscillations and negative spikes reaching -50 V. This behavior reflects the removal of one string from the original five. Similarly, the current (I_{PV}) in the optimal case stabilizes near 360 A, whereas the fault condition leads to a significant reduction, settling around 150–200 A.

results at Boost converter level

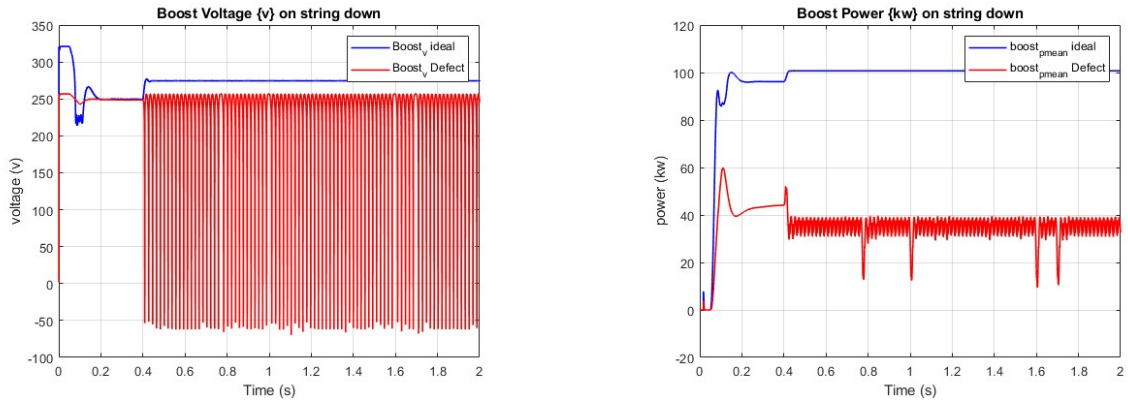

(a) Boost voltage

(b) Boost Power

Figure 3.8: Boost converter results at string down

The power and voltage curves for the boost converter give a good look at how the fault plays out. For the power ($P_{\text{mean boost}}$), it holds steady around 100 kW in the optimal case after a quick rise, but drops sharply to about 30–40 kW with some jitter in the fault scenario, showing the impact of losing a string. The voltage (V_{boost}) The results of this curve exhibit a perfect alignment with the previously obtained curve (V_{PV}), Figure 3.7.

results at grid level

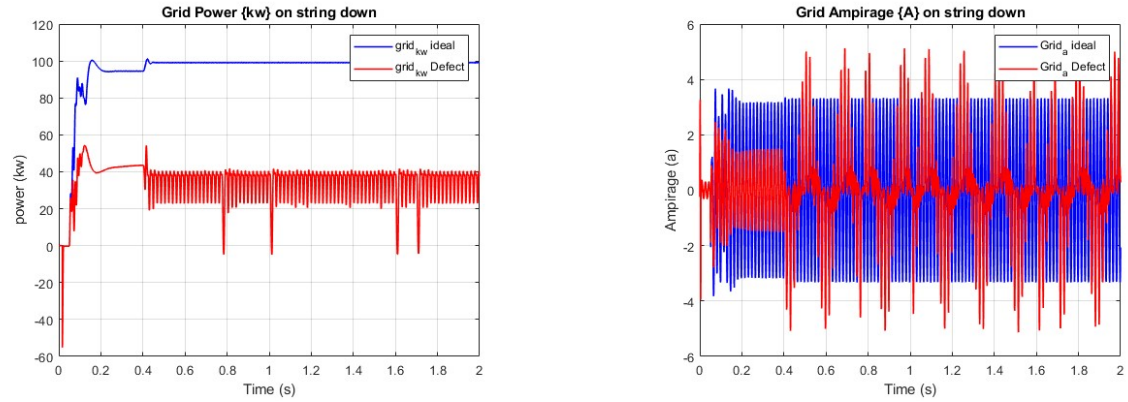

(a) Grid Power

(b) Grid ampirage

Figure 3.9: Grid results at string down

The power and current curves for the grid, related to the first fault, reveal significant differences between the optimal and defective conditions. For the power (P_{grid}) the results of this curve exhibit a perfect alignment with the previously obtained curve ($P_{\text{mean\_boost}}$), Figure 3.8. The current (A_{grid}) maintains a steady oscillation around 0 A in the optimal scenario, but the fault introduces an early spike and more erratic behavior, indicating instability in power delivery.

3.3.1.2 Change in solar irradiance

The second fault we simulated involves a change in solar irradiance, where it suddenly drops from 1000 to 300 at a specific moment before climbing back up. This causes the voltage and current at the PV array to dip noticeably during the low irradiance phase, reflecting less power generation, then recover as the irradiance returns to normal. In real life, this could happen due to passing clouds , reducing the sunlight hitting the panels and lowering their output until conditions improve again.

results at pv arry level

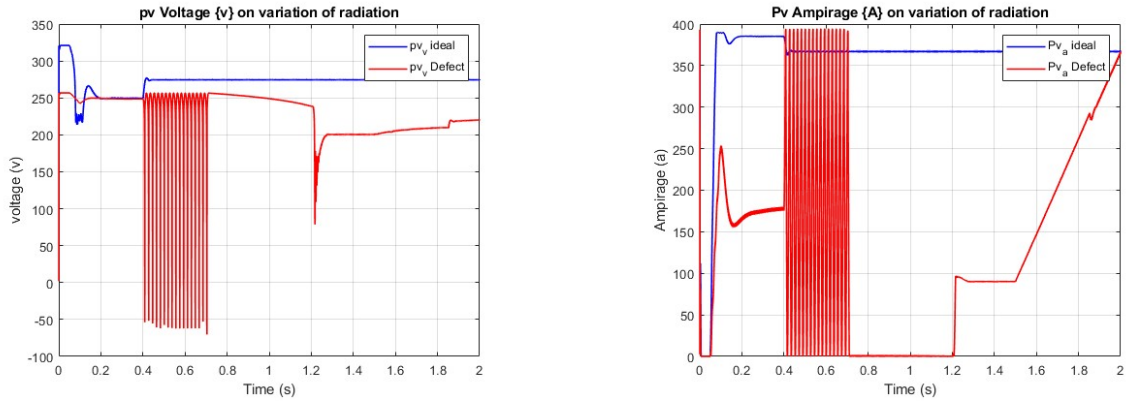

(a) PV voltage

(b) PV amperage

Figure 3.10: PV arry results at change in solar irradiance

The voltage (V_{PV}) in a sudden decrease in solar radiation drops to 250 V with oscillation, then drops to approximately 200 V. The current and voltage curves for the PV array show a clear effect from the change in solar irradiance. The current (I_{PV}) during the fault drops sharply to about 170 A with oscillation, then the value goes down to 0 A followed by a sudden peak.

results at Boost converter level

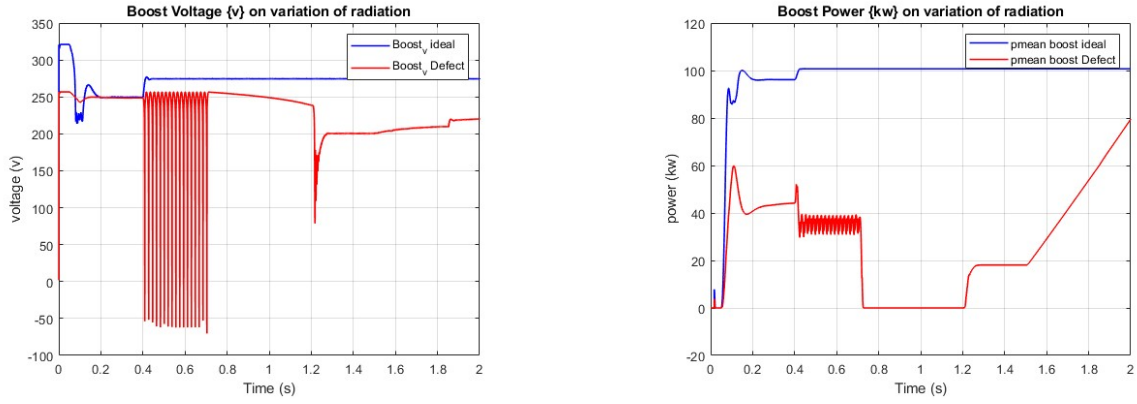

(a) Boost voltage

(b) Boost Power

Figure 3.11: Boost converter results at change in solar irradiance

The power curve ($P_{\mathrm{mean\_boost}}$) for the boost converter. Under the fault condition, the power drops sharply to around 20–30 kW when the irradiance decreases to 300, then

gradually recovers as it returns to 1000, indicating a temporary reduction in power output. The voltage (V_{boost}) curve exhibits a perfect alignment with the previously obtained curve (V_{PV}), Figure3.10.

results at grid level

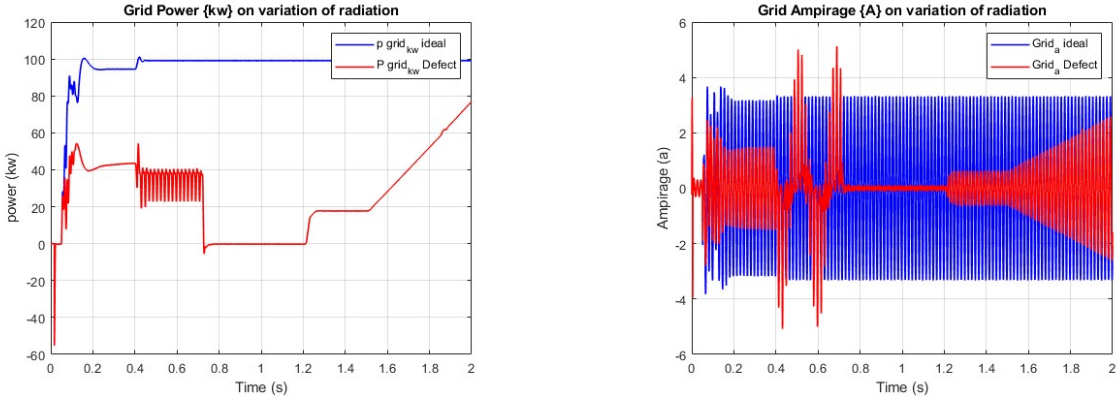

(a) Grid Power

(b) Grid ampirage

Figure 3.12: Grid results at change in solar irradiance

For the power (P_{grid}), it causes a significant drop to around 20–30 kW when irradiance falls to 300, followed by a gradual recovery as it returns to 1000. The current (A_{grid}) during the fault exhibits a noticeable spike and increased fluctuations during the low irradiance period, settling back as conditions normalize.

3.3.2 Boost converter

3.3.2.1 open Circuit

The fault simulated at the boost converter level involves setting a constant input of 0 to the transistor gate, effectively rendering it non-operational to emulate an open-circuit fault. This condition halts the converter's functionality, resulting in a complete cessation of voltage and current output from the boost stage. Under normal operation, the converter efficiently steps up the voltage and sustains power flow, whereas this fault leads to an output of zero, interrupting energy transfer to downstream components such as the grid. In practical terms, this scenario could arise from a failure in the control signal or a malfunctioning transistor, potentially due to an open circuit from a severed connection or damaged component, thereby severely compromising the system's power delivery capability.

- results at pv arry level

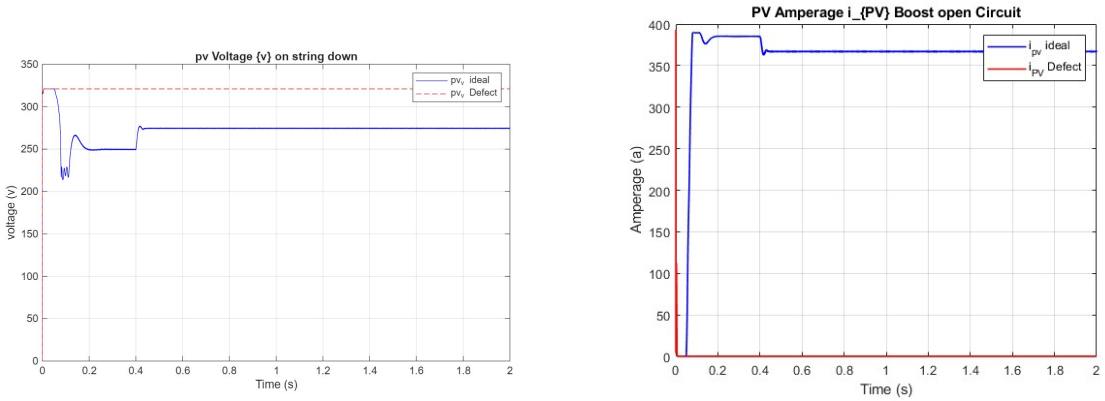

(a) PV voltage (b) PV amperage

Figure 3.13: PV arry results at Boost open circuit

The voltage (V_{PV}) under the fault rises up to 330 V and stabilizes, indicating no effective power conversion. For the current (I_{PV}), the condition shows a rapid decline to near zero, reflecting the cessation of current flow due to the inactive transistor.

- results at Boost converter level

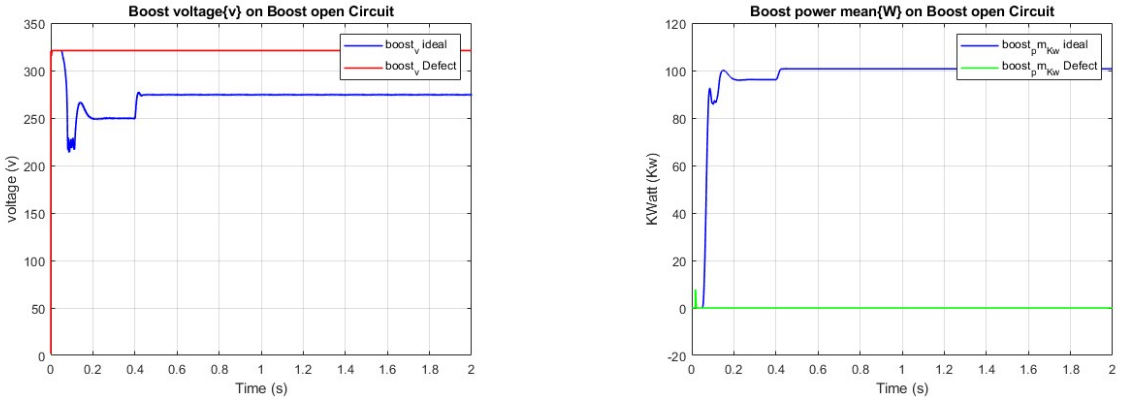

(a) Boost voltage (b) Boost Power

Figure 3.14: Boost converter results at Boost open circuit

The voltage (V_{Boost}) declines sharply and remains negligible, reflecting the cessation of voltage conversion. The power ($P_{\text{mean boost}}$) drops sharply to 0 kW following the initial rise, reflecting the complete cessation of power output.

- results at grid level

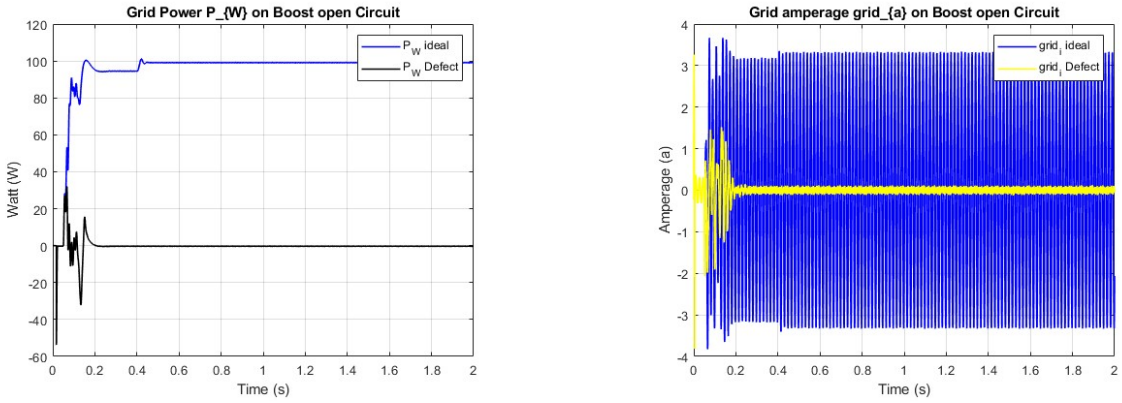

(a) Grid Power (b) Grid ampirage

Figure 3.15: Grid results at Boost open circuit

For the power (P_{grid}), indicating a complete cessation of power delivery due to the inactive transistor. Similarly, the current (A_{grid}) under the fault shows an initial spike followed by a drop to near 0 A.

3.3.2.2 Short Circuit

In this simulation we changed the value of 0 to 1 in order to simulate a short circuit fault and compare it with an open circuit fault.

- results at pv arry level

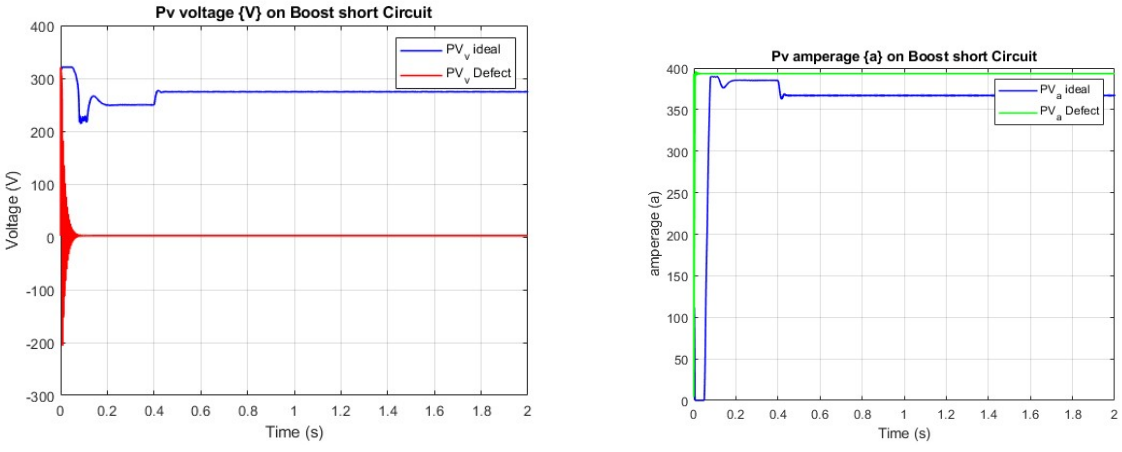

(a) PV voltage (b) PV amperage

Figure 3.16: PV arry results at Boost Short circuit

The voltage (V_{PV}), in the fault condition, causes a sharp drop to around -200 V, indicating a reversal due to the uncontrolled conduction of the transistor. The current curve (A_{PV}) rises up to 400 A and stabilizes.

- results at Boost converter level

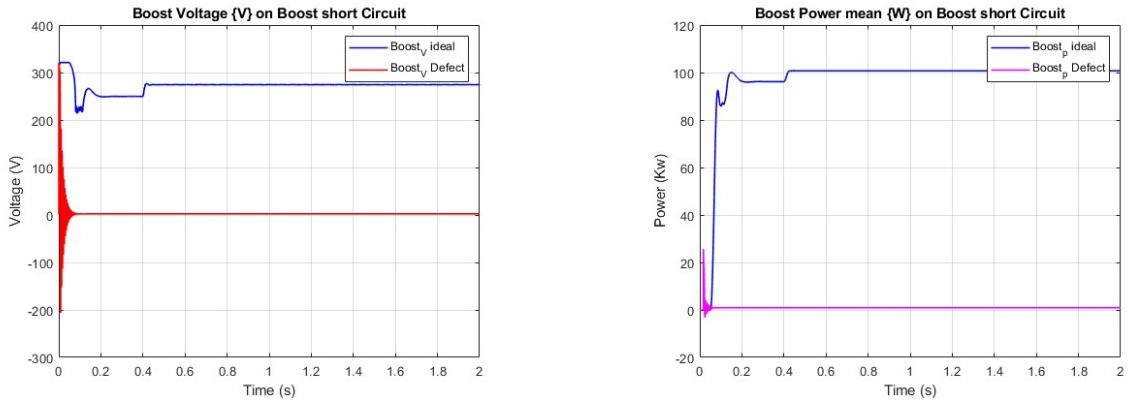

(a) Boost voltage (b) Boost Power

Figure 3.17: Boost converter results at Boost Short circuit

The power ($P_{\text{mean boost}}$) under the fault declines sharply to zero, indicating a complete loss of power. And the voltage (V_{boost}) curve exhibits a perfect alignment with the previously obtained curve (V_{PV}), Figure3.16.

- results at grid level

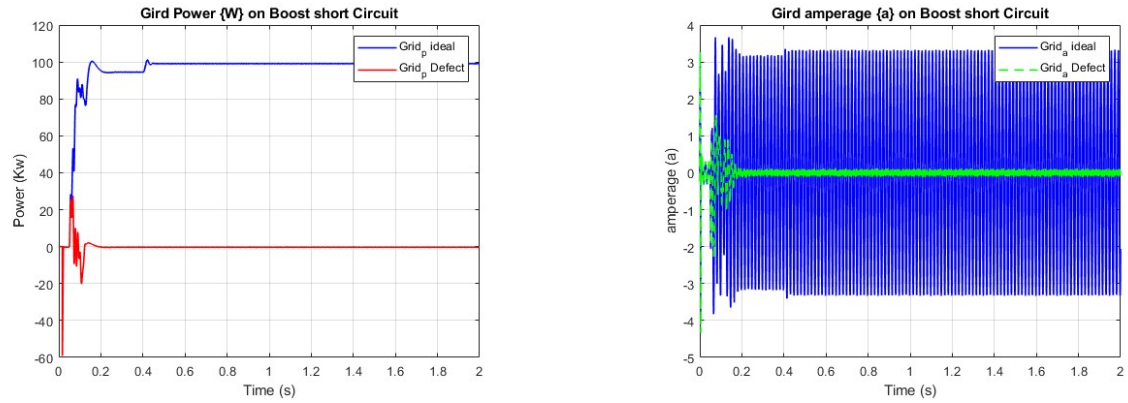

(a) Grid Power (b) Grid ampirage

Figure 3.18: Grid results at Boost Short circuit

The power (P_{grid}), it indicating a complete loss of power delivery due to the uncontrolled transistor state. Similarly, the current (A_{grid}) under the fault, it exhibits an initial spike followed by a stabilization near 0A.

3.3.3 Grid

3.3.3.1 Grid off

The fault simulated at the grid level involves disconnecting the system from the grid, effectively isolating it from the network. In a real-world scenario, this could occur due to a deliberate disconnection for maintenance, a tripped circuit breaker, or a failure in the grid interface, resulting in a complete halt of power delivery to the network and potentially affecting the system's operational stability.

– results at pv arry level

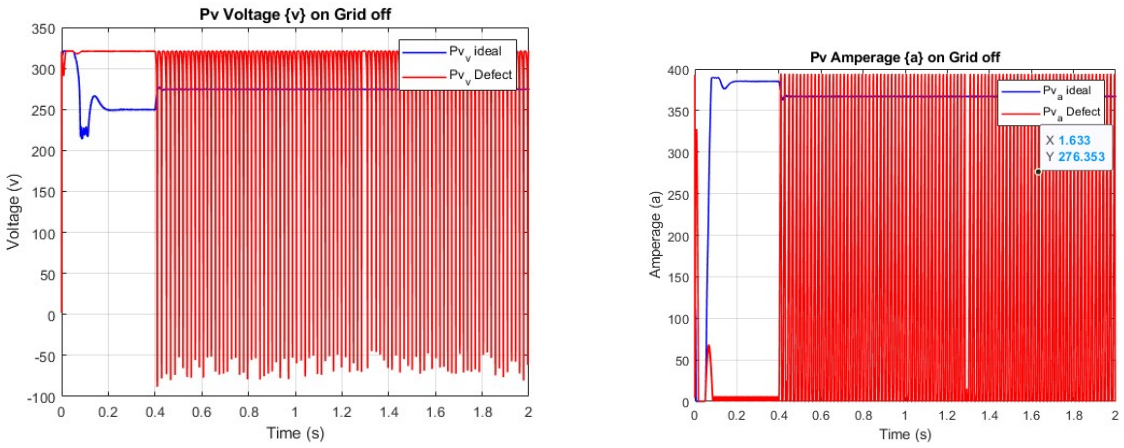

(a) PV voltage (b) PV amperage

Figure 3.19: PV arry results at Grid off

For the voltage (V_{PV}), shows a significant drop to around −50–100 V with pronounced oscillations. The current (I_{PV}) declines sharply to near 0 A, reflecting the absence of power export to the grid.

- results at Boost converter level

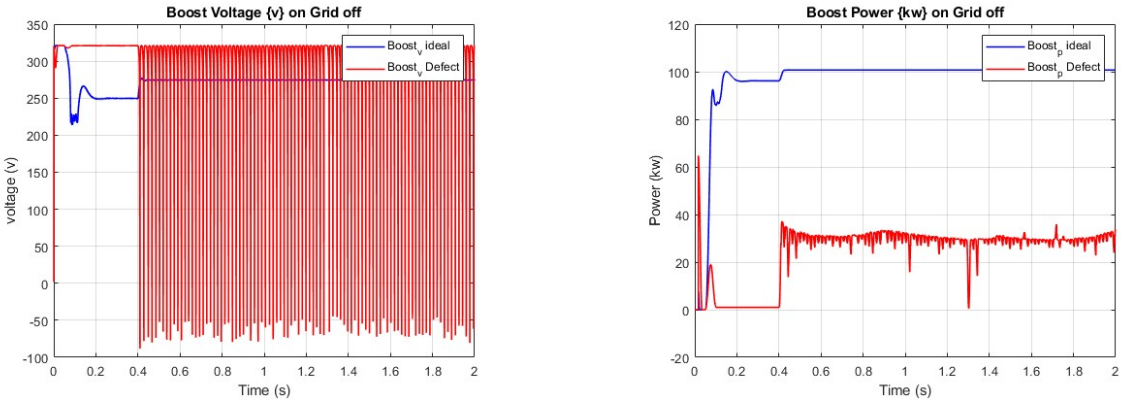

(a) Boost voltage (b) Boost Power

Figure 3.20: Boost converter results at Grid off

The power on the fault condition results in a sharp decline to around 20–40 kW with significant oscillations, reflecting the loss of grid load and subsequent instability. The voltage (V_{boost}) curve exhibit a perfect alignment with the previously obtained curve (V_{PV}), Figure3.19.

- results at grid level

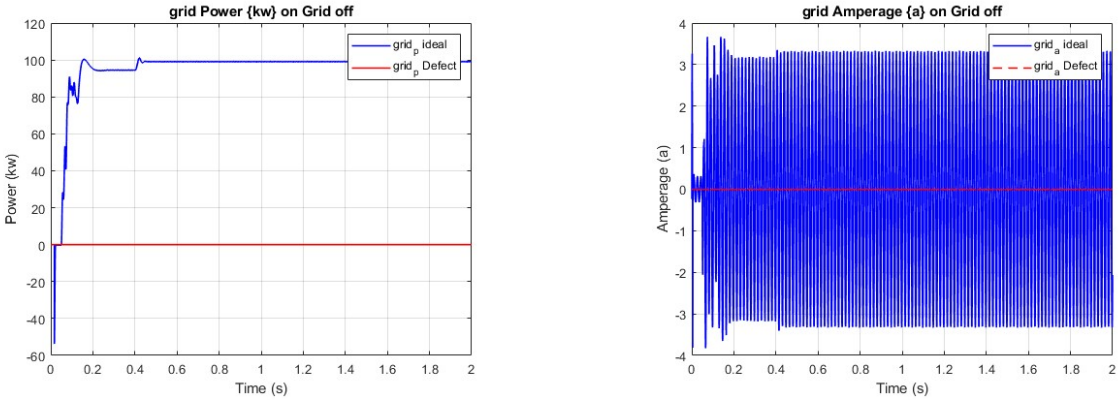

(a) Grid Power

(b) Grid ampirage

Figure 3.21: Grid results at Grid off

For the power (P_{grid}), it drops sharply to 0 kW due to the disconnection. Similarly, the current (I_{grid}) stabilizes at approximately 0 A, reflecting the absence of current flow to the network.

3.3.3.2 Phase down

The second fault simulated at the grid level involves a phase dropout, where one of the connected phases to the grid is intentionally disconnected. In a real-world context, this could occur due to a phase failure, a broken connection, or a fault in the grid interface, leading to an unbalanced power delivery and potential instability in the system's grid integration.

  - results at pv arry level

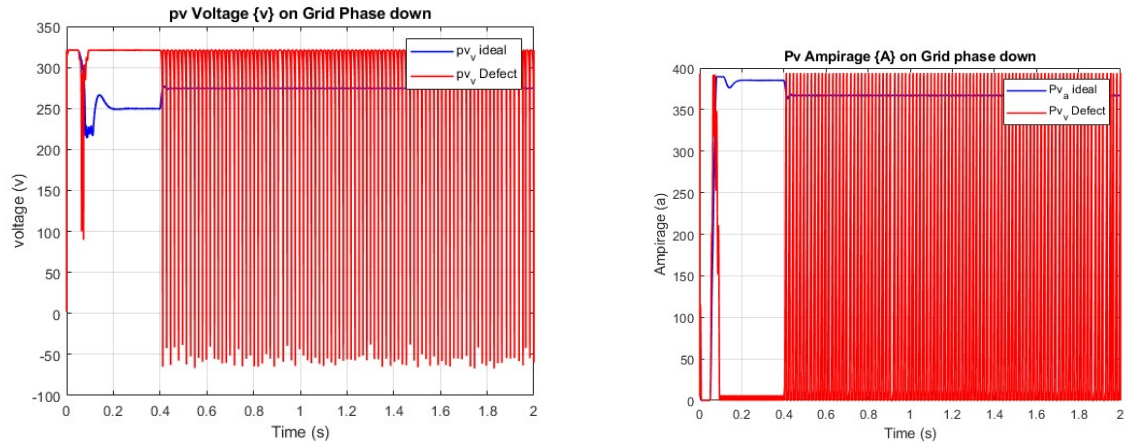

(a) PV voltage (b) PV amperage

Figure 3.22: PV arry results at Phase down

The voltage on the fault condition results in a significant drop to around -50 V with noticeable oscillations, reflecting the imbalance caused by the loss of one phase. Similarly, the current (A_{PV}), it declines sharply to near 0 A.

- results at Boost converter level

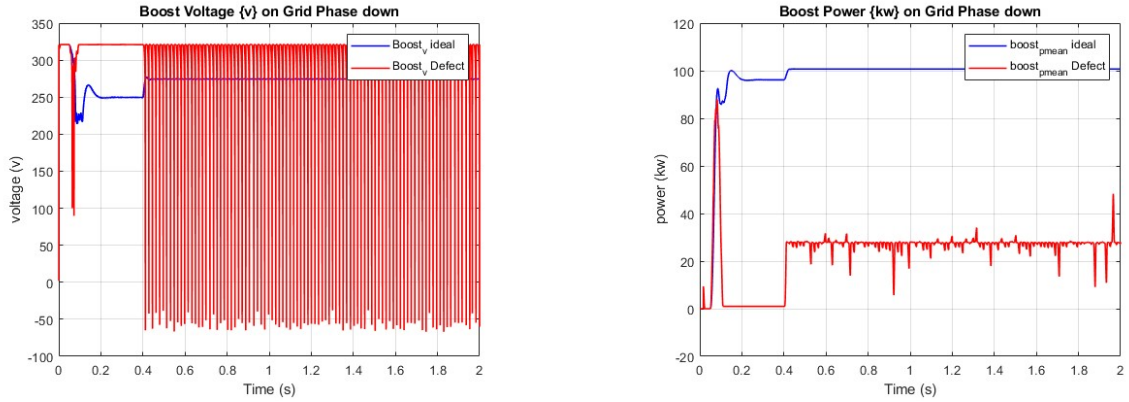

(a) Boost voltage (b) Boost Power

Figure 3.23: Boost converter results at Phase down

For the power ($P_{\text{mean boost}}$), it drops sharply to around 20–40 kW with pronounced oscillations. The voltage (V_{boost}) curve exhibits a perfect alignment with the previously obtained curve (V_{PV}), Figure 3.22.

- results at grid level

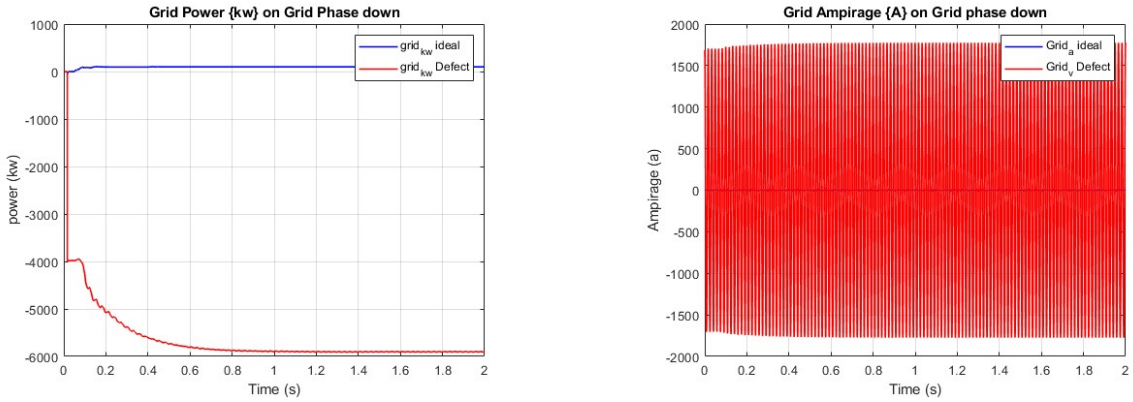

(a) Grid Power

(b) Grid ampirage

Figure 3.24: Grid results at Phase down

The power (P_{grid}), it drops sharply to approximately -5000 kW due to the loss of one phase. Similarly, the current (A_{grid}) shows extreme fluctuations, reaching values up to 2000 A and dropping to -2000 A, reflecting a highly unbalanced and erratic current flow.

3.4 Conclusion

This chapter analyzed various fault scenarios in a 100 kW grid-connected PV system using MATLAB/Simulink. Faults at the PV array, boost converter, and grid levels were simulated and compared to the optimal case. Each fault significantly impacted system performance, with power, voltage, and current dropping sharply in most cases. The results consistently showed a strong correlation between different system stages, confirming the reliability of the simulation model. These findings highlight the importance of fault detection and form a foundation for enhancing system resilience in future research.

General Conclusion

The growing adoption of photovoltaic (PV) systems as a sustainable energy solution brings with it the critical challenge of maintaining system efficiency and reliability over time. While PV technology offers numerous advantages—such as modularity, environmental benefits, and decreasing costs—it remains vulnerable to various faults that can significantly reduce its performance. These faults, whether at the PV array level, the power electronics interface, or the grid connection, often lead to measurable power losses that compromise both energy yield and economic return.

This study has demonstrated that analyzing power losses is an effective approach for detecting and diagnosing faults in grid-connected PV systems. Through detailed modeling and simulation using MATLAB/Simulink, a 100kW PV system was evaluated under optimal and faulty operating conditions. Faults were introduced at different points of the system, including string disconnections, boost converter failures, and grid disturbances. By comparing voltage, current, and power outputs between normal and fault conditions, distinct behavioral patterns were identified—enabling precise detection of anomalies and their probable causes.

The results confirm that power loss analysis can serve as a practical and non-invasive tool for real-time fault monitoring. It provides a strong foundation for developing intelligent control and diagnostic algorithms, especially in the context of large-scale PV installations. Integrating such fault detection mechanisms enhances not only the system's operational stability but also supports the broader transition to sustainable and resilient energy infrastructures.

Future work can explore real-time implementation using embedded systems, artificial intelligence for fault classification, and experimental validation under varying weather conditions. These advancements will be crucial in ensuring the long-term viability and reliability of solar power as a major contributor to global energy supply.

Bibliography

[1] REN21, "Renewables 2024 Global Status Report," Paris, France, 2024.

[2] E. Skoplaki and J. A. Palyvos, "On the temperature dependence of photovoltaic module electrical performance: A review of efficiency/power correlations," *Solar Energy*, vol. 83, no. 5, pp. 614–624, 2009.

[3] Y. Kim, H. Lee, and B. Cho, "A fault detection and diagnosis scheme for photovoltaic systems using a normalized power difference and fuzzy logic," *Solar Energy*, vol. 180, pp. 62–76, 2019.

[4] R. Ahmad, G.-M. Muntean, and M. Z. H. Bhuiyan, "A comprehensive study of renewable energy sources: Classifications, challenges and suggestions," *Energy Strategy Reviews*, vol. 43, p. 100939, 2022.

[5] International Energy Agency, *Global Energy Review 2025*. IEA, 2025.

[6] International Renewable Energy Agency (IRENA), "Renewable capacity highlights 2025," Mar. 2025.

[7] E. Graham, N. Fulghum, and K. Altieri, "Global electricity review 2025," Apr. 2025.

[8] J. A. Gubner, *Probability and Random Processes for Electrical and Computer Engineers*. Cambridge, UK: Cambridge University Press, 2024.

[9] M. K. W. (2025) 3 types of pv system. https://www.scribd.com. [Online]. Available: https://www.scribd.com.

[10] S. Seba, M. Birane, and K. Bennouiza, "A comparative analysis of boost converter topologies for photovoltaic systems using maximum power point (p&o) and beta methods under partial shading," *Rev. Roum. Sci. Techn.–Électrotechn. et Énerg.*, vol. 68, no. 4, pp. 375–380, 2023.

[11] F. Blaabjerg, Ed., *Control of Power Electronic Converters and Systems*. London, U.K.: Academic Press, 2018, vol. 1.

[12] M. A. Elgendy, B. Zahawi, and D. J. Atkinson, "Assessment of the incremental conductance maximum power point tracking algorithm," *IEEE Trans. Sustain. Energy*, vol. 4, no. 1, pp. 108–117, 2013.

[13] S. Jain and V. Agarwal, "Comparison of the performance of maximum power point tracking schemes applied to single-stage grid-connected photovoltaic systems," *IET Electr. Power Appl.*, vol. 1, no. 5, pp. 753–762, 2007.

[14] X. Li *et al.*, "An improved mppt method for pv system with fast-converging speed and zero oscillation," *IEEE Trans. Ind. Appl.*, vol. 52, no. 6, pp. 5051–5064, 2016.

[15] N. Femia *et al.*, *Power Electronics and Control Techniques for Maximum Energy Harvesting in Photovoltaic Systems*. CRC Press, 2012.

[16] X. Li *et al.*, "Enhanced variable step-size p&o mppt for pv systems," *Sci. Rep.*, vol. 15, p. 11700, 2025.

[17] M. Birane *et al.*, "Smart inverters for grid stability," *IEEE Trans. Sustain. Energy*, vol. 10, no. 2, pp. 691–698, 2019.

[18] A. Harrag *et al.*, "Mppt techniques for pv systems: A review," *Energies*, vol. 16, no. 5, p. 2206, 2023.

[19] R. Bisht *et al.*, "Ann-based mppt for pv systems," *Sci. Rep.*, vol. 14, p. 18280, 2024.

[20] S. Jain *et al.*, "Robust vs-p&o mppt for wind/pv hybrids," *Energies*, vol. 24, no. 5, p. 731, 2022.

[21] M. Islam *et al.*, "Grid integration challenges of photovoltaic systems," *IEEE Trans. Sustain. Energy*, vol. 11, no. 3, pp. 1859–1871, 2020.

[22] IEEE, "IEEE Standard 1547-2018, "IEEE Standard for Interconnection of Distributed Energy Resources"," 2018.

[23] J. Smith *et al.*, "Smart inverter functions for pv grid integration," *Renew. Sustain. Energy Rev.*, vol. 82, pp. 3090–3101, 2018.

[24] A. Johnson *et al.*, "Voltage regulation in pv-rich distribution networks," *IEEE Trans. Power Del.*, vol. 34, no. 2, pp. 827–836, 2019.

[25] S. Davis, *Grid Integration of Solar Photovoltaics*. Academic Press, 2022.

[26] R. Brown *et al.*, "Derms for high-penetration pv scenarios," *IEEE Access*, vol. 9, pp. 45 621–45 634, 2021.

[27] J. H. Wohlgemuth *et al.*, "Long-term reliability of pv modules," in *Proc. IEEE PVSC*, 2013, pp. 0015–0020.

[28] F. J. Montes-Romero *et al.*, "Mechanical reinforcement solutions for pv frames," *Eng. Struct.*, vol. 252, p. 113508, 2022.

[29] K. Osmani, A. Haddad, T. Lemenand, B. Castanier, M. Alkhedher, and M. Ramadan, "A critical review of pv systems faults with the relevant detection methods," *Energy Nexus*, vol. 12, p. 100257, Dec. 2023.

[30] S. Abd and E. Gharabawy, "Review on corrosion in solar panels," *Int. J. Smart Grid*, vol. 2, p. 218, 2018.

[31] S. Sarikh, M. Raou, A. Bennouna *et al.*, "Photovoltaic discoloration and cracks: experimental impact on the iv curve degradation," in *Proc. 9th Int. Renewable Energy Congress (IREC)*, Hammamet, Tunisia, 2018, p. 60916.

[32] R. Mahalakshmi, M. Karuppasamypandiyan, A. Bhuvanesh *et al.*, "Classification and detection of faults in grid connected photovoltaic system," *Int. J. Sci. Eng. Res.*, vol. 7, pp. 149–154, 2016.

[33] M. Köntges *et al.*, "Quantifying hotspot risk in pv modules," *IEEE J. Photovoltaics*, vol. 8, no. 2, pp. 532–538, 2018.

[34] E. Batzelis, K. Samaras, G. Vokas *et al.*, "Off-grid inverter faults: diagnosis, symptoms and cause of failure," *Mater. Sci. Forum*, vol. 856, pp. 315–321, 2016.

[35] A. Y. Appiah, X. Zhang, B. B. K. Ayawli, and F. Kyeremeh, "Review and performance evaluation of photovoltaic array fault detection and diagnosis techniques," *Int. J. Photoenergy*, vol. 2019, 2019.

[36] G. Artale *et al.*, "Dc series arc faults in pv systems. detection methods and experimental characterization," in *24th IMEKO TC4 Int. Symp. and 22nd Int. Workshop on ADC and DAC Modelling and Testing (IWADC)*, 2020, pp. 135–140.

[37] J. H. Wohlgemuth *et al.*, "Bypass diode reliability," in *Proc. IEEE PVSC*, 2019.

[38] R. G. Vieira, F. M. U. de Araújo, M. Dhimish, and M. I. S. Guerra, "A comprehensive review on bypass diode application on photovoltaic modules," *Energies*, vol. 13, no. 10, 2020.

[39] K. AbdulMawjood, S. S. Refaat, and W. G. Morsi, "Detection and prediction of faults in photovoltaic arrays: A review," in *2018 IEEE 12th Int. Conf. on Compatibility, Power Electronics and Power Engineering (CPE-POWERENG)*, 2018.

[40] M. Chang, C. Chen, C. Hsueh, W. Hsieh, E. Yen, and K. Ho, "The reliability investigation of pv junction box based on 1gw worldwide field database," in *Proc. 42nd IEEE Photovoltaic Specialist Conf. (PVSC)*, 2015.

[41] M. K. Alam, F. Khan, and M. A. Bhuiyan, "Detection, location, and diagnosis of different faults in large solar pv system—a review," *Int. J. Low-Carbon Technol.*, vol. 18, pp. 573–595, 2023.

[42] S. Z. Said, S. Z. Islam, N. H. Radzi, C. W. Wekesa, M. Altimania, and J. Uddin, "Dust impact on solar pv performance: A critical review of optimal cleaning techniques for yield enhancement across varied environmental conditions," *Energy Reports*, vol. 12, 2024.

[43] A. M. B. P. R. M. S. C. Lazzaretti *et al.*, "A monitoring system for online fault detection and classification in photovoltaic plants," *Sensors*, vol. 20, no. 17, p. 4688, 2020.

[44] W. Chine *et al.*, "A novel fault diagnosis technique for photovoltaic systems based on artificial neural networks," *Renew. Energy*, vol. 90, pp. 501–512, 2016.

[45] S. Silvestre, A. K. da Silva, M. A. Chouder, D. Guasch, and E. Karatepe, "New procedure for fault detection in grid connected pv systems based on the evaluation of current and voltage indicators," *Energy Convers. Manage.*, vol. 86, pp. 241–249, 2014.

[46] IEC, "Photovoltaic (pv) systems - testing, documentation and maintenance requirements - part 3: Photovoltaic modules and plants - outdoor infrared thermography," IEC 62446-3:2017, 2017.

[47] S. Silvestre *et al.*, "Review of techniques for fault detection in pv systems," *IEEE J. Photovoltaics*, vol. 10, no. 3, pp. 914–926, 2020.

[48] A. M. B. P. R. M. S. C. Lazzaretti *et al.*, "Arc fault detection in photovoltaic systems using wavelet transforms," *IEEE Trans. Sustain. Energy*, vol. 11, no. 3, pp. 1831–1839, 2020.

[49] F. M. A. Khan *et al.*, "A comprehensive review of fault diagnosis in photovoltaic systems," *Renew. Sustain. Energy Rev.*, vol. 151, p. 111536, 2021.

[50] Q. Hu, Z. He, H. Li, Y. Chen, and X. Wang, "Real-time fault detection for pv systems using empirical mode decomposition," *IEEE Trans. Ind. Electron.*, vol. 65, no. 5, pp. 4285–4294, 2018.